UNIVERSIDAD DE CANTABRIA

Facultad de Ciencias

DIFUSIÓN ELECTROMAGNÉTICA POR UNA NANOPARTÍCULA METÁLICA: RÉGIMEN DE CAMPO CERCANO

(Electromagnetic scattering by a metallic nanosphere: near field regime)

Trabajo de Fin de Grado
para acceder al

GRADO EN FÍSICA

Autor: Beatriz Menéndez López

Director: Fernando Moreno Gracia

Co-Director: Alfredo Franco Pérez

Septiembre - 2020

Resumen

Para entender la interacción radiación-materia de una nanoesfera metálica cuando es iluminada por una onda plana electromagnética, se han utilizado aproximaciones dipolares y la teoría de Mie. Primero, revisando los modelos de tipo dipolo y su validez en el rango de la nanoescala, y luego, analizando la respuesta óptica de una esfera de oro de 20 nm de radio cuando es iluminada por una onda plana de $\lambda = 550$ nm. El cálculo nuérico de los campos difundidos se realizó con el software matemático MatLab. En particular, este trabajo se centra en el comportamiento del campo electromagnético en las proximidades de la nanoesfera, es decir, en la región de campo cercano. En esta región se observan propiedades extraordinarias debidas a las ondas evanescentes generadas por resonancias plasmónicas.

Palabras clave: Difusión, nanoesfera metálica, aproximación dipolar, campo cercano, plasmones

Abstract

Dipole approximations and Mie theory were used to understand the radiation-matter interactions of a metallic nanosphere when it is illuminated by a plane electromagnetic wave. First, dipole models and its validity in the nanoscale range were revised, then , the optical response of a 20 nm radius gold sphere was analysed when it is illuminated by a plane electromagnetic wave of $\lambda = 550$ nm. The scattered fields were calculated using MatLab software. In particular, this work focuses the attention on the electromagnetic behaviour in the proximity of the particle, the near field region, which has exceptional properties due to evanescent waves generated by plasmon resonances.

Keywords: Scattering, metal nanosphere, dipole approximation, near field, plasmons

Contents

Chapter 1

Introduction

One typical way to deal with a problem in physics is going from the simplest case to more challenging cases. Solving a simpler version of a problem can be extremely helpful to set up the basis to figure out more complex cases. A good example of this methodology is depicted in reference [1], which concerns the plasmonic behaviour in the UV wavelength range. This has inspired the spirit of my research to get the results I am going to show in this manuscript.

This research is focused on the field scattered by a spherical nanoparticle embedded in electromagnetic radiation, especially its behaviour on the scattering in the vicinity of the particle surface.

The introduction chapter covers briefly the importance of nanoscience to contextualise before we get started, the fundamentals of radiation-matter interaction, the essential problem of this work, and the objectives. Along Chapter *2* the basis of Mie theory and Mie scattering field equations are explained, leading up to the analysis of scattering coefficients and the evolution of efficiency parameters as a function of the wavelength. In Chapter *3* some approximations are introduced and analysed to simplify the calculus, for instance, the pure dipole approximation and its validity range as function of the particle size. The Chapter also contains a comparative between the complete calculation of the scattered field by the Mie theory and the result obtained by the approximation of a pure single dipole. Chapter *4* digs into the study of the near electric field to study the electric field and the flux of energy in the proximity of the sphere surface.

Chapter *5* closes the work gathering up the conclusions of the analysis, the milestones of nanotechnology, and the future work in this field. Besides, an appendix contains the computing code in MatLab, created to calculate and visualize the fields from the theoretical equations.

1.1. Nanoscale, properties, and applications

Nanoscience is not only the study of the world in the nanoscale which involves nanometric structures, i.e, structures which characteristic size is around few nanometers ($1\ nm = 10^{-9}\ m$). The importance of nanoscale resides in the ability to manipulate and characterize the properties of matter at the level of single atoms, which has lead to the discovery that nanoscale structures often have unique and different physical properties with respect to the same matter

on the bulk scale [2].

These structures, smaller than approximately 100 nm can be for example single molecules, so nanoscale also deals with the molecular range. As nanoscale is comparable with molecular dimensions (see *Figure 1.1*), the study of nanoscience has taken an important role in medicine and health researches. From an optical point of view, the special features of nanomatter are not negligible at the subwavelength scale.

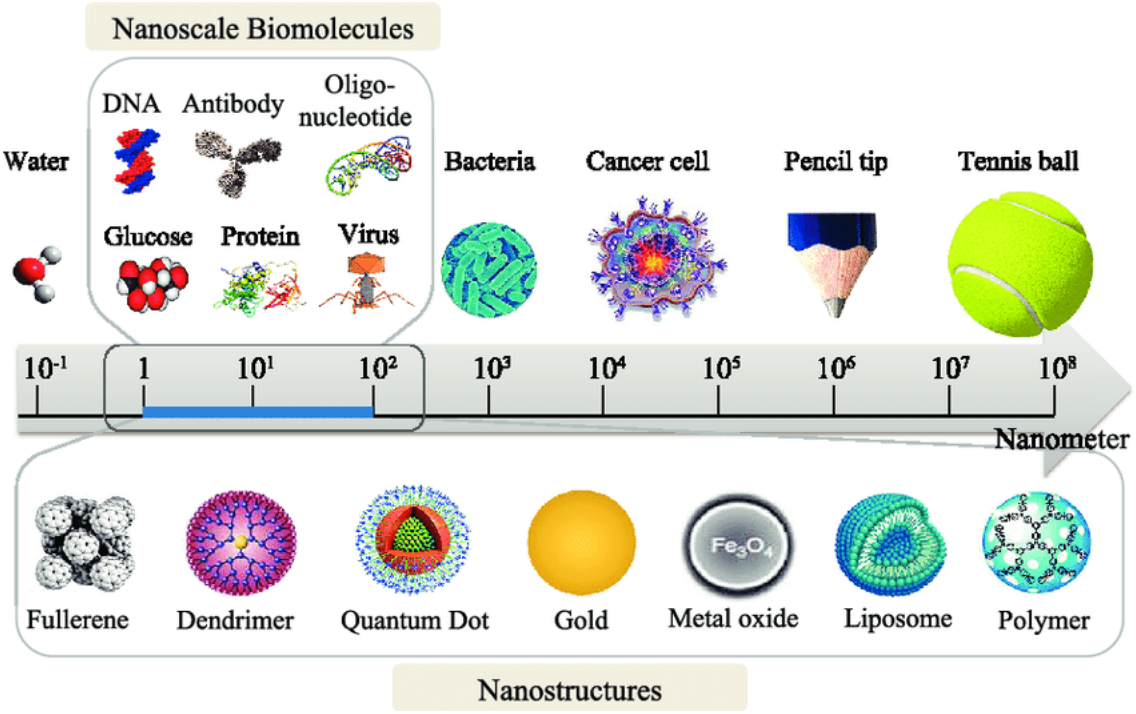

Figure 1.1: Nanoscale scheme of biomolecules and nanostructures [3].

1.1.1. Evanescent waves

One outstanding optical property observed when the structures are smaller than the illumination wavelength (λ), is the evanescent electromagnetic waves phenomenon, which is intimately related to the near field optics.

When the electromagnetic field interacts with a metal nanoparticle, it excites the conducting electrons leading to electronic plasma oscillations driven by the incident electric field [4]. At resonance, the phenomenon is called "plasmon", a quasi-particle created by those collective oscillations of electrons. This term has been coined by Pines in 1956 after he studied the electronic plasma oscillations [5].

The electromagnetic radiation bound to the surface at the interface between a metal and a dielectric are known as surface plasmons which are sustained by electromagnetic waves decaying evanescently in the direction perpendicular to the interface. Another type of plasmonic response is that excited around a nanostructure when the wavelength is much bigger than the size of the particle, these are called localised surface plasmons (LSPs).

Here, it can be seen that plasma physics and optics have existed separately for a long time, but after the definition of plasmon and surface plasmons, both fields of study have overlapped creating a prolific link between them. Furthermore, Drude's model and Mie theory still belong to the theoretical basis of the actual studies of localised surface plasmons. Surface plasmons and plasma modes are connected by similar physics, the dispersion relation is the same despite the difference in electron number density. "Hence, by reaching back as far as primordial earth (for terrestrial gaseous plasmas) and the 4th century AD (for plasmons in solid plasmas) and looking forward to the state-of-the-art nanomedical and technological advances, one concludes that everything old, is ultimate, new once again." [6].

To understand better the concept of evanescent waves, it is useful to look at the total internal reflection phenomenon:

When light travels through a medium and is reflected from the interface with a less dense medium at an angle higher than the critical angle, light suffers total internal reflection, as can be observed at the left side of *Figure 1.2*. However, on the right side of this figure, it can be shown that when a material of similar refractive index is brought into close proximity to the reflecting surface, part of the light is transmitted to the material, leaving a partial reflection in the prism.

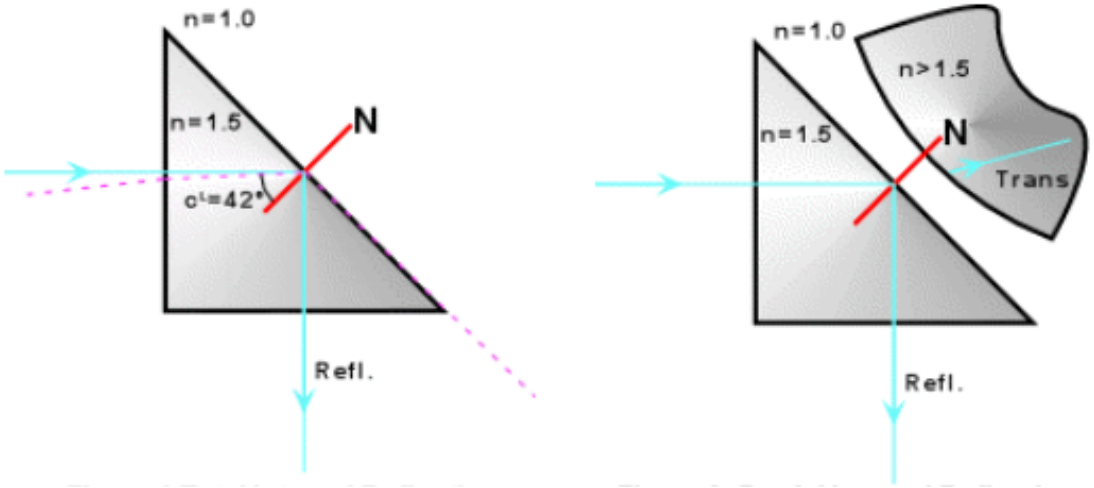

Figure 1.2: Total internal reflection (left) in a glass prism. Partial internal reflection (right) in a glass prism near to another material of similar refractive index [7].

This phenomenon proves that an evanescent field is traveling through the small gap of air, reaching the material next to the prism.

Those sort of waves can be created by total internal reflection, a metallic rough surface or a confined surface, like a sphere; the origin of those waves is different, but the wave itself has the similar electromagnetic properties. Evanescent waves are non propagating inhomogeneous waves which propagate along the surface. This is represented in *Figure 1.3*. Throughout this work the surface will be a metallic sphere surface. In addition, evanescent waves are localised waves that enhance the near field in the proximities of the metal-dielectric interface by the resonant excitation of surface plasmons, allowing for instance, the enhancement of the Raman

Scattering leading to surface enhance spectroscopy techniques like SERS(Surface Enhanced Raman Spectroscopy) or assisting photocatalytic processes, very interesting, for instance for Hydrogen production or elimination of CO_2. Also, these surface plasmonic phenomena are very attractive for industrial, medical an other applications (see *Section 1.1.3*).

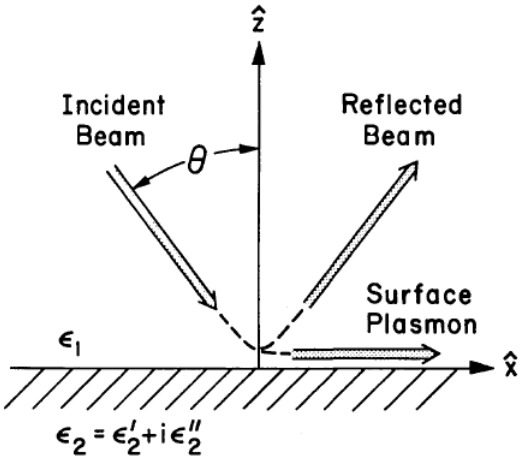

Figure 1.3: Scheme of the excitation of a surface plasmon wave [8].

1.1.2. State of the art

Nanoscience has appeared as a powerful field of investigation, but some of their concepts have been used throughout history, for instance nanoscience concepts are present in the Lycurgus cup which dates back to the $4th$ century. This masterpiece has gold or gold-silver alloy nanoparticles within the glass to induce the amazing dichroism effect that it is shown in *Figure 1.4*, [9].

Figure 1.4: Lycurgus cup viewed in reflected light (left image) and transmitted light (right image), © The Trustees of the British Museum

Despite the ancient use of nanoparticles in the Lycurgus cup, stained glass windows or in Damascus saber blades, their properties had not been studied until the mid-nineteenth century and understood right up to the twentieth century.

This study field begins when Faraday looked into light scattering properties of gold colloidal solutions [10]. Nowadays, there are very important investigation fields as nanophotonics and nanoplasmonics, focused on manipulating and characterizing nanostructures for chemical, biomedical, environmental, and industrial purposes.

Nanophotonics studies the interaction of photons with nanostructures and its behaviour, mixing branches as optics and nanotechnology. Nanoplasmonics is a branch of nanophotonics which deal with optical phenomena in nanoscale metal systems. Standing out the ability to concentrate energy on the nanoscale due to surface plasmons [11].

Despite the evolution in this field investigations, there are currently published works related to the behaviour of dipoles, for instance the emission of circularly polarized light by a linear dipole has been recently reported in reference [12]; that means that the dipole, considered as an approximation to solve more complex problems, is also an active subject of study. Furthermore, despite the incredible optical properties obtained with nanoscience, there is a time gap between the lab experiments and basic research and their implementation in industrial applications. However, the only way to progress is to continue investigating and acquiring knowledge at the nanoscale level taking basic models based on very well known concepts such as the electric dipole as we will see all along this research.

1.1.3. Applications

Nanoparticles are highly regarded in many industrial sectors, but metal nanoparticles, in particular, have unique optical properties due to the localised surface plasmon resonance (LSPR) being a very valuable resource in many research areas [13].

A very active research area in medicine is the implementation of plasmonic gold nanoparticles for photothermal therapy and cancer diagnosis, where nanoparticles are excited by a resonant frequency of light, and the localised surface plasmons generated at the surface of the nanoparticles are expected to kill surrounding cells by thermal dissipation [14].

The best conditions to enhance the sensitivity of a sensor based in nanoplasmonics are reached when the evanescent field reaches its maximum amplitude and confinement [15]. Nanostructures such as periodical nanohole arrays or surface-immobilized nanoparticles can be used to detect changes in their dielectric environment, e.g. refractive index changes. This enables the determination of kinetic and thermodynamic data for different molecular events, especially on biomolecular targets. This type of sensing is very useful in cancer cell detection or macromolecular interactions characterization, among others [16] [17].

The characterization of the optical properties of the nanoparticles is usually based on the study of their optical absorption, reflection and photoluminescence. Photocatalysis is another application of metallic nanoparticles, they help to change the velocity of a chemical reaction when they are illuminated by electromagnetic radiation. As plasmonic nanoparticles have the

ability to absorb and scatter light from a broad part of the spectrum, they are very useful also in photocatalysis, either introducing more light to reactions with photosensitive materials, e.g. polymerizations; inducing hot electrons for molecular bindings or heating up to increase the velocity of the reactions [18].

In Raman spectroscopy, a LASER beam suffers inelastic scattering when it interacts with a sample. The frequency variation allows to calculate the resonance frequency of the material, and plot the spectrum which displays the molecular vibrations and contains information about the sample which could be useful to identify not only crystals but also amorphous, liquids, gaseous samples, etc.

An important application in the near field is Surface Enhanced Raman Spectroscopy (SERS), a surface-sensitive resonance extension of Raman spectroscopy, in which the sample is placed on metal or semiconductor substrates. SERS also present bioanalytical applications, allowing to analyse biological materials like blood, body fluids, or even DNA. What is more, gold and silver nanoparticle solutions are used in combination with SERS to detect fingerprints [19].

One of the newest applications is related to photovoltaic cells and solar vapor generation. Plasmonic structures can offer ways of reducing the thickness of the photovoltaic absorber layers, thus reducing costs while also increasing their efficiency. For example, metallic nanoparticles can be used as subwavelength scattering elements converting free plane waves into surface plasmons trapped in thin absorber layers [20]. On the other hand, the plasmon-enhanced solar vapor generation is a photothermal phenomenon that is being used to induce the liquid-vapor phase change of water by solar energy [21].

There are many more applications of metallic nanoparticles in drugs, mechanical industries or energy harvesting, but mentioning all of them could fill an entire book [22].

1.2. Radiation-matter interaction

To study how the electromagnetic field is in the vicinity of a nanosphere, it is necessary to understand how the metallic nanoparticle behaves in response to an incident plane electromagnetic wave, that is, the interaction between radiation and matter.

An electromagnetic wave consists in oscillating electric and magnetic fields propagating through space. As the matter is composed of electric charges, when it is illuminated by an electromagnetic wave, the charges oscillate, mainly due to their interaction with the electric field of the wave; those excited charges can absorb part of the energy carried by the wave and transform it into other forms of energy or redistribute the energy through space by scattering.

The attenuation of the amplitude of an electromagnetic wave by its interaction with matter is known as **extinction**. It is due to both the scattering and the absorption produced by the interaction between the electromagnetic wave and matter. The scattering and absorption of a plane electromagnetic wave by a sphere is described by Mie theory, which was formulated in the early 20th century as an analytical solution to the Maxwell equations for an isotropic

and homogeneous spherical particle illuminated by a plane wave.

The study of the behaviour of the electromagnetic radiation interacting with a sphere which size is shorter than the wavelength radiation is possible thanks to Mie theory. Solving this problem with the simplest geometry makes it possible to implement it in more complex scenarios, letting look into a wide variety of nanostructures and their response to the light.

1.3. The problem and its geometry

The electromagnetic waves are solutions of Maxwell equations but they can be expressed analytically only for few cases. Besides, the solutions greatly depend on the geometrical symmetries of each case. In the case of a homogeneous and isotropic metal sphere embedded in time dependent electromagnetic fields, the waves can be calculated through the sum of successive corrections to an approximated solution. In this work, the approximated solutions are compared to the corrected ones.

On account of that, the selected problem of this work consists of a homogeneous and isotropic gold nanosphere which center is at the origin of the coordinates system, surrounded by vacuum, and an incident electromagnetic wave (linearly polarized in $x-$axis) which propagates along the vertical direction, $z-$axis.

In order to achieve representations of the fields, it is necessary to apply the coordinate conversion from spherical polar coordinates to cartesian coordinates according the next set of equations:

$$\left.\begin{aligned} \hat{x} &= \sin\theta\cos\phi\ \ \hat{r} + \cos\theta\cos\phi\ \ \hat{\theta} - \sin\phi\ \ \hat{\phi} \\ \hat{y} &= \sin\theta\sin\phi\ \ \hat{r} + \cos\theta\sin\phi\ \ \hat{\theta} + \cos\phi\ \ \hat{\phi} \\ \hat{z} &= \cos\theta\ \ \hat{r} - \sin\theta\ \ \hat{\theta} \end{aligned}\right\} \tag{1.1}$$

The cartesian coordinates x, y and z are described in spherical polar coordinates as a function of r, θ and phi. The variable r represents the radial coordinate; the polar angle θ is the angle between the the zenit direction (the $z-$ axis) and the radial coordinate; and azimutal angle ϕ is the projection of the radial coordinate in $x-y$ plane, starting in the $x-$ axis. As it is shown in the *Figure 1.5*, where a plane electromagnetic wave travels in the positive direction of the z axis and the electric field oscillates along the $x-$ axis.

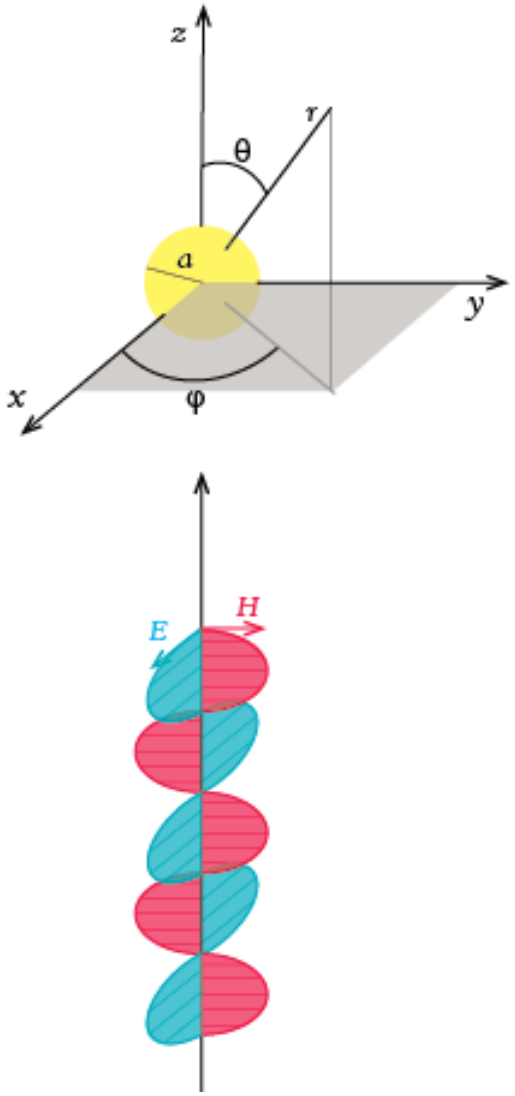

Figure 1.5: Scheme of a gold nanoparticle with spherical polar (r, θ, ϕ) and cartesian coordinates (x, y, z), the direction of the electric and magnetic field, and propagation of light. The radius of the sphere is named as a.

A plane electromagnetic wave is named linearly polarized when the electric field oscillates in a given plane within the direction of propagation. In this case, it has been chosen the $x-$polarization with the direction of propagation in the $z-$axis. It means that the wave propagates through the $z-$direction, the electric field oscillates in $x-$axis, and the magnetic field perpendicular to both of them, that is on $y-$axis.

The solutions of the Maxwell equations depend on the materials refractive index which is the main optical property of the materials and describes through the electric permittivity ε and the magnetic permeability, μ. Those values are characteristic of each material, but they are also wavelength dependant, therefore, it is important to evaluate the problem for an enough wide wavelength spectral interval to get a better idea of the material optical behaviour.

The complex refractive index is defined in such a way that it includes both the refractive index of the matter and its extinction coefficient. It is the addition of the refractive index (real part), n, and the extinction coefficient (imaginary part), κ, as stated in *Eq* (1.2).

$$N = n + i \cdot \kappa \tag{1.2}$$

$$\varepsilon = N^2 = (n + i \cdot \kappa)^2 \tag{1.3}$$

The extinction coefficient, κ, indicates the amount of attenuation when the electromagnetic wave propagates through the material, so the extinction coefficient is related to the absorption and to the scattering, as well as to the electric permittivity, as it is stated in *Eq* (1.3).

1.4. Motivation and main objectives

This work pretends to dig in the field scattered by a nanosphere when it is illuminated with a plane electromagnetic wave. In particular, paying attention to the optical response in the near field, which has exceptional properties for the potential applications mentione above.

The key goals of this work are:

- To compute the electric field based on the Mie theory and to study the contribution of the scattering coefficients.
- To compute the electric field through the dipole approximation.
- To compare the electric field in each case, and to determine their validity range.
- To focus on the near field.

The computing system used all over the work was MatLab, which is a computing environment specialized in matrix manipulations and function plots.

The main objective of this work is to understand the electromagnetism in the vicinity of a nanoparticle. The study of the field scattering is based on Mie theory, and it is compared with a calculus for dipole models to confirm its validity and to determine the limit of the approximations.

It is noteworthy that the calculus all over this work is for a gold nanosphere, but it works for every metallic nanosphere. Gold is used as a relevant example of metallic nanosphere because it is commonly used for health applications due to its inert chemical properties and its biocompatible features.

Chapter 2

Mie theory

Throughout this chapter, Mie theory is presented as the theoretical tool to calculate the complete scattered field by a small sphere of arbitrary radius and refractive index, embedded in vacuum. The equations are analyzed thoroughly below, following the guidelines of Bohren and Huffman [23].

The scattered field can be calculated as a superposition of normal modes, and each one of them weighted by their corresponding scattering coefficient. Therefore, the scattered field can be understood by studying the values and the contributions of the scattering coefficients and their associated normal modes as will be shown in *Section 2.1*. In this way some physical quantities can be obtained, like the scattering cross section, as it is done in *Section 2.2*.

To determine the electromagnetic fields, Mie theory [23] starts from the definition of two vectors, $\mathbf{M}$ and $\mathbf{N}$. They are the electromagnetic normal modes of a spherical particle, which meet the next requirements: their divergence is zero as follows from *Eq* (2.1), the curl of $\mathbf{M}$ should be proportional to $\mathbf{N}$, the curl of $\mathbf{N}$ should be proportional to $\mathbf{M}$, as the *Eq* (2.2) states, and both must satisfy the vector wave equation (2.3). $\mathbf{N}$ is associated to the electric type normal modes, and $\mathbf{M}$ is associated to the magnetic ones.

$$\mathbf{M} = \nabla \times (\mathbf{r}\psi) \tag{2.1}$$

$$\mathbf{N} = \frac{\nabla \times (\mathbf{M})}{k} \tag{2.2}$$

$$\nabla^2\mathbf{M} + k^2\mathbf{M} = 0 \tag{2.3}$$

where $\mathbf{r}$ is the radius vector, ψ a scalar function, and k is the wave vector defined as a function of the wavelength λ:

$$k = \frac{2 \cdot \pi}{\lambda} \tag{2.4}$$

A vector function satisfies the vector wave equation if the scalar function ψ is a solution to the scalar wave equation

$$\nabla^2\psi + k^2\psi = 0 \tag{2.5}$$

A particular form of the solution to the wave equation in spherical polar coordinates (Ψ) is composed by a radial R, azimuthal Θ and an angular Φ function which depend on the coordinates r, θ and ϕ respectively:

$$\Psi(r, \theta, \phi) = R(r) \cdot \Theta(\theta) \cdot \Phi(\phi) \tag{2.6}$$

The Mie theory provides ψ solutions for spherical symmetry that can be expanded as infinite series functions, known as generating functions

$$\left.\begin{aligned}\psi_{emn} &= \cos m\phi \cdot P_n^m(cos\theta) \cdot z_n(kr) \\ \psi_{omn} &= \sin m\phi \cdot P_n^m(cos\theta) \cdot z_n(kr)\end{aligned}\right\} \tag{2.7}$$

which work to describe the vector spherical harmonics:

$$\left.\begin{aligned}\mathbf{M_{emn}} &= \nabla \times (\mathbf{r} \cdot \psi_{emn}) \\ \mathbf{M_{omn}} &= \nabla \times (\mathbf{r} \cdot \psi_{omn}) \\ \mathbf{N_{emn}} &= \frac{\nabla \times (\mathbf{M}_{emn})}{k} \\ \mathbf{N_{omn}} &= \frac{\nabla \times (\mathbf{M}_{omn})}{k}\end{aligned}\right\} \tag{2.8}$$

The subscripts e and o denote even and odd, which comes from the solutions of the wave equation. The subscripts n and m indicate the degree and the order, respectively of the Legendre Polynomials (P_n^m) and the spherical Bessel functions $z_n(\rho)$, which are defined in *Eq* (2.29) and *Eq* (2.20). In *Eq* (2.7), r, θ and ϕ are the spherical polar coordinates, being the scalar function ψ the solution of the scalar wave equation for spherical symmetry.

Eq (2.7) allow to express the plane $x-$polarized wave in terms of spherical polar coordinates and expand it in vector harmonics.

$$E_i = E_0 \cdot e^{ikr\cos\theta}\hat{\mathbf{x}} \tag{2.9}$$

Eq (2.9) represents a plane $x-$polarized wave, with E_i as the incident plane wave and E_0 as the amplitude of the vector. While *Eq* (2.10) represents the same kind of wave but in terms of vector spherical harmonics, with B and A as coefficients associated to the magnetic and the electric modes, respectively.

$$E_i = \sum_{m=0}^{\infty}\sum_{n=m}^{\infty}(B_{emn}\mathbf{M_{emn}} + B_{omn}\mathbf{M_{omn}} + A_{emn}\mathbf{N_{emn}} + A_{omn}\mathbf{N_{omn}}) \tag{2.10}$$

Thus any linearly polarized plane electromagnetic wave may be expressed as a linear combination of the vector spherical harmonics.

In a similar way, the fields inside and outside the sphere are described by the Mie theory as analysed thoroughly in *Section 2.1*.

2.1. Mie Scattering

The fields scattered by a sphere, electrical and magnetic, are given by

$$E_s = \sum_{n=1}^{\infty} E_n \cdot \left(i \cdot a_n \cdot N_{e1n}^{(3)} - b_n \cdot M_{o1n}^{(3)}\right) \tag{2.11}$$

$$H_s = \sum_{n=1}^{\infty} E_n \cdot \left(i \cdot b_n \cdot N_{o1n}^{(3)} - a_n \cdot M_{e1n}^{(3)}\right) \tag{2.12}$$

where $E_n = i^n \cdot E_0 \cdot \frac{2n+1}{n(n+1)}$ being $n = 1, 2, 3...$, a_n and b_n are the scattering coefficients, and the superscript (3) means that the spherical Bessel function $z_n(\rho)$, is the spherical Hankel function of first order $h_n^{(1)}$ (see *Eq* (2.20)).

To understand equations *Eq* (2.11) and *Eq* (2.12) every term is discussed below:

Scattering coefficients

For each value of n, there are two types of modes, the transverse magnetic modes and the transverse electrical modes. Magnetic and electric normal modes are weighted by the scattering coefficients a_n and b_n respectively. That means, the coefficients a_a are the amplitudes of the oscillations of magnetic type, and b_n are the amplitudes of electric oscillations.

$$a_n = \frac{m \cdot \psi_n(m \cdot x) \cdot \psi_n'(x) - \psi_n(x) \cdot \psi_n'(m \cdot x)}{m \cdot \psi_n(m \cdot x) \cdot \xi_n'(x) - \xi_n(x) \cdot \psi_n'(m \cdot x)} \tag{2.13}$$

$$b_n = \frac{\psi_n(m \cdot x) \cdot \psi_n'(x) - m \cdot \psi_n(x) \cdot \psi_n'(m \cdot x)}{\psi_n(m \cdot x) \cdot \xi_n'(x) - m \cdot \xi_n(x) \cdot \psi_n'(m \cdot x)} \tag{2.14}$$

The size parameter (x) relates the radius of the sphere (a) with the wavelength (λ) of the incident electromagnetic wave as follows.

$$x = k \cdot a = \frac{2 \cdot \pi \cdot N \cdot a}{\lambda} \tag{2.15}$$

In *Eq* (2.13) and *Eq* (2.14) the m represents the relative refractive index which is obtained from the refractive indexes of the sphere (ε_1) and of the surrounding media (ε_m), as it is written in *Eq* (2.16).

$$m = \frac{N_1}{N} = \sqrt{\frac{\varepsilon_1}{\varepsilon_m}} \tag{2.16}$$

Besides, the scattering coefficients also involve Riccati-Bessel functions

$$\psi_n(\rho) = \rho \cdot j_n(\rho) \tag{2.17}$$

$$\xi_n(\rho) = \rho \cdot h_n^{(1)}(\rho) \tag{2.18}$$

$$\rho = k \cdot r \tag{2.19}$$

composed by Spherical Bessel functions of the third kind or spherical Hankel functions of the first order

$$h_n^{(1)}(\rho) = j_n(\rho) + i \cdot y_n(\rho) \tag{2.20}$$

being j_n and y_n Spherical Bessel functions

$$j_n(\rho) = \sqrt{\frac{\pi}{2 \cdot \rho}} \cdot J_{n+\frac{1}{2}}(\rho) \tag{2.21}$$

$$y_n(\rho) = \sqrt{\frac{\pi}{2 \cdot \rho}} \cdot Y_{n+\frac{1}{2}}(\rho) \tag{2.22}$$

where $J_{n+\frac{1}{2}}$ is a Bessel function of the first kind and $Y_{n+\frac{1}{2}}$ is a Bessel function of the second kind.

Analysis of scattering coefficients

Data for the relative refractive index m has been obtained from [24] in order to calculate the respective scattering coefficients for a gold nanosphere of 20 nm radius, in a wavelength range between 300 nm to 800 nm. It is interesting to analyse this problem for a nanosphere of around 20 nm because for this particle size, several approximations can be made to solve the problem by different ways.

By replacing this data in *Eq* (2.13) and *Eq* (2.14), and taking n from 1 to 10, it is noted that each scattering coefficient is smaller than the previous one, being the most relevant the coefficient with lowest n values as it can be shown in *Figure 2.1*, where coefficients a and b are represented for the first two values of n.

To understand correctly *Figure 2.1*, it must be taken into account that the ordinate axis is in logarithmic scale, having orders of magnitude of difference between coefficients. It is also remarkable the behaviour around $\lambda = 525$ nm, which can correspond to a resonance phenomenon.

As the scattered fields are directly proportional to the scattering coefficients (see *Eq* (2.11) and *Eq* (2.12)), the greater the value of the coefficients, the greater their contribution to the calculated field. To sum up, the calculus of the fields is almost complete only considering the first terms in *Eq* (2.11) and *Eq* (2.12), where a_1 is the most relevant coefficient, and the next terms are smaller and smaller[25].

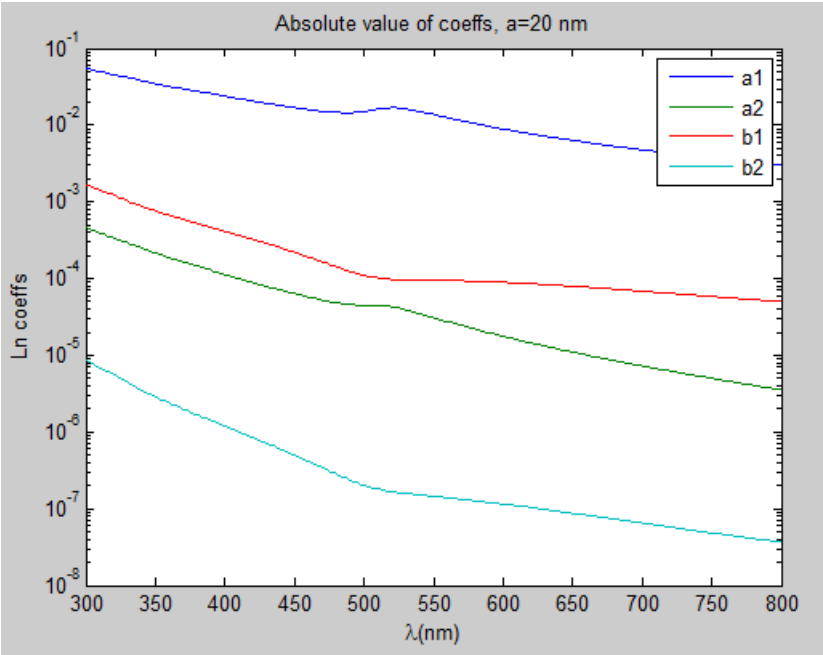

Figure 2.1: Comparison of the coefficients in a logarithmic scale in the wavelength range between 300 *to* 800 nm.

Electromagnetic normal modes

As the sphere is a body bounded by a close surface, there can be set up a system of standing waves, allowing to represent the electric field patterns (in *Figure 2.2*) on the surface of a sphere concentric with the particle. The magnetic field pattern can be obtained by the rotation of the electric field pattern by rotating 90° the azimuthal angle.

The electromagnetic normal modes of a spherical particle may be written as infinite series of the vector spherical harmonics as *Eq* (2.23) to *Eq* (2.26) show.

$$\begin{aligned} M_{o1n} = &\cos\phi \cdot \pi_n(\cos\theta) \cdot z_n(\rho) \cdot \hat{\mathbf{e}}_\theta \\ &- \sin\phi \cdot \tau_n(\cos\theta) \cdot z_n(\rho) \cdot \hat{\mathbf{e}}_\phi \end{aligned} \tag{2.23}$$

$$\begin{aligned} M_{e1n} = &-\sin\phi \cdot \pi_n(\cos\theta) \cdot z_n(\rho) \cdot \hat{\mathbf{e}}_\theta \\ &- \cos\phi \cdot \tau_n(\cos\theta) \cdot z_n(\rho) \cdot \hat{\mathbf{e}}_\phi \end{aligned} \tag{2.24}$$

$$\begin{aligned} N_{o1n} = &\sin\phi \cdot n \cdot (n+1) \cdot \sin\theta \cdot \pi_n(\cos\theta) \cdot \frac{z_n(\rho)}{\rho} \cdot \hat{\mathbf{e}}_\mathbf{r} \\ &+ \sin\phi \cdot \tau_n(\cos\theta) \cdot \frac{[\rho \cdot z_n(\rho)]'}{\rho} \cdot \hat{\mathbf{e}}_\theta \\ &+ \cos\phi \cdot \pi_n(\cos\theta) \cdot \frac{[\rho \cdot z_n(\rho)]'}{\rho} \hat{\mathbf{e}}_\phi \end{aligned} \tag{2.25}$$

$$\begin{aligned} N_{e1n} = &\cos\phi \cdot n \cdot (n+1) \cdot \sin\theta \cdot \pi_n(\cos\theta) \cdot \frac{z_n(\rho)}{\rho} \cdot \hat{\mathbf{e}}_\mathbf{r} \\ &+ \cos\phi \cdot \tau_n(\cos\theta) \cdot \frac{[\rho \cdot z_n(\rho)]'}{\rho} \cdot \hat{\mathbf{e}}_\theta \\ &+ \sin\phi \cdot \pi_n(\cos\theta) \cdot \frac{[\rho \cdot z_n(\rho)]'}{\rho} \cdot \hat{\mathbf{e}}_\phi \end{aligned} \tag{2.26}$$

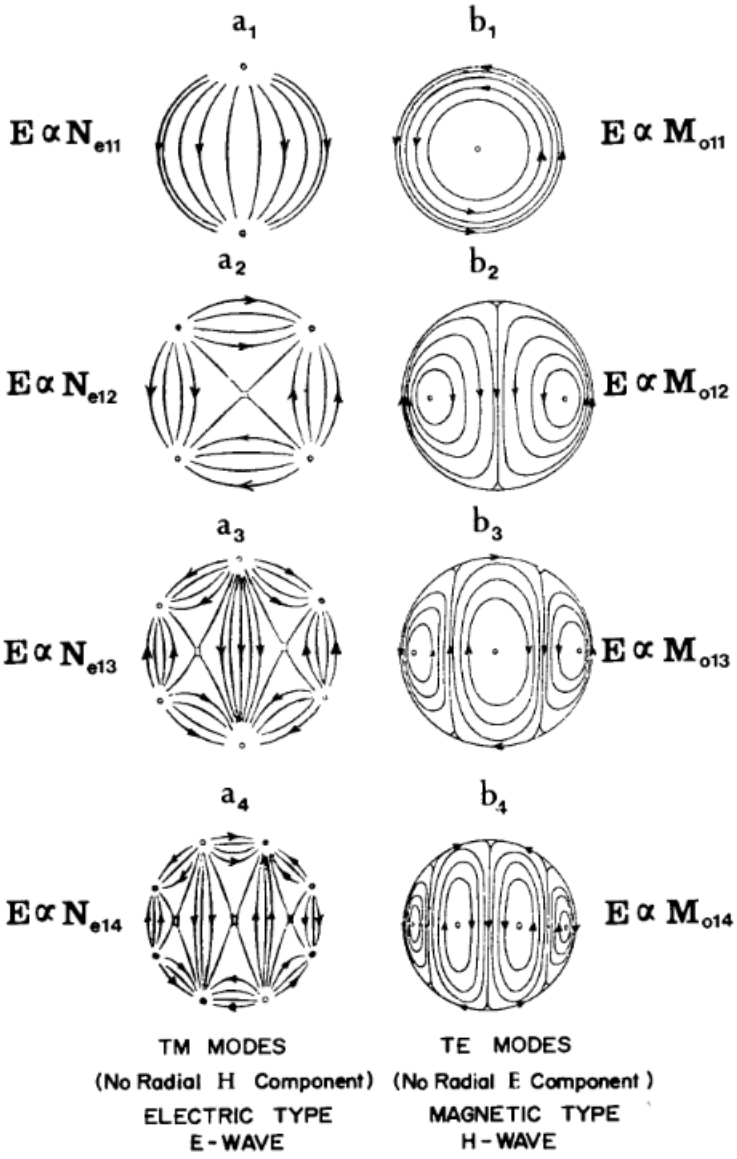

Figure 2.2: Representation of first four electric normal modes [26]

Normal modes are related to Angle-dependent functions, and those, in turn, with Legendre Polynomials.

$$\pi_n = \frac{P_n^1}{\sin\theta} \tag{2.27}$$

$$\tau_n = \frac{\partial P_n^1}{\partial\theta} \tag{2.28}$$

$P_n^m(\mu)$ are the associated Legendre polynomials with degree n and order m,

$$P_n^m(\mu) = (1-\mu^2)^{m/2}\frac{\partial^m P_n(\mu)}{\partial\mu^m} \tag{2.29}$$

$\mu = \cos\theta$, P_n are the Legendre polynomials, and for this work, m is considered as 1.

2.2. Cross sections comparison and influence of coefficients

Cross section is an effective area that is defined by the amount of energy that interacts with the sphere. Whenever the incident energy contained in an area is equal to the total energy scattered, this area is considered the scattering cross section.

Extinction, absorption, and scattering cross sections can be calculated by using the scattering coefficients in the following equations:

$$C_{sca} = \frac{2\pi}{k^2} \sum_{n=1}^{\infty} (2n+1)(|a_n|^2 + |b_n|^2) \tag{2.30}$$

$$C_{ext} = \frac{2\pi}{k^2} \sum_{n=1}^{\infty} (2n+1) Re(a_n + b_n) \tag{2.31}$$

$$C_{ext} = C_{abs} + C_{sca} \tag{2.32}$$

Therefore, their corresponding efficiency is defined as the cross section per unit of area

$$\left.\begin{aligned} Q_{ext} &= \tfrac{C_{ext}}{\pi \cdot a^2} \\ Q_{sca} &= \tfrac{C_{sca}}{\pi \cdot a^2} \\ Q_{abs} &= Q_{ext} - Q_{abs} \end{aligned}\right\} \tag{2.33}$$

where a is the sphere radius as it is shown in *Figure 1.5*

After determining the cross sections for some sphere radius values, they can be compared as in the figure below, where it has been used only the first three terms of the sum in *Eq* (2.30) and *Eq* (2.31).

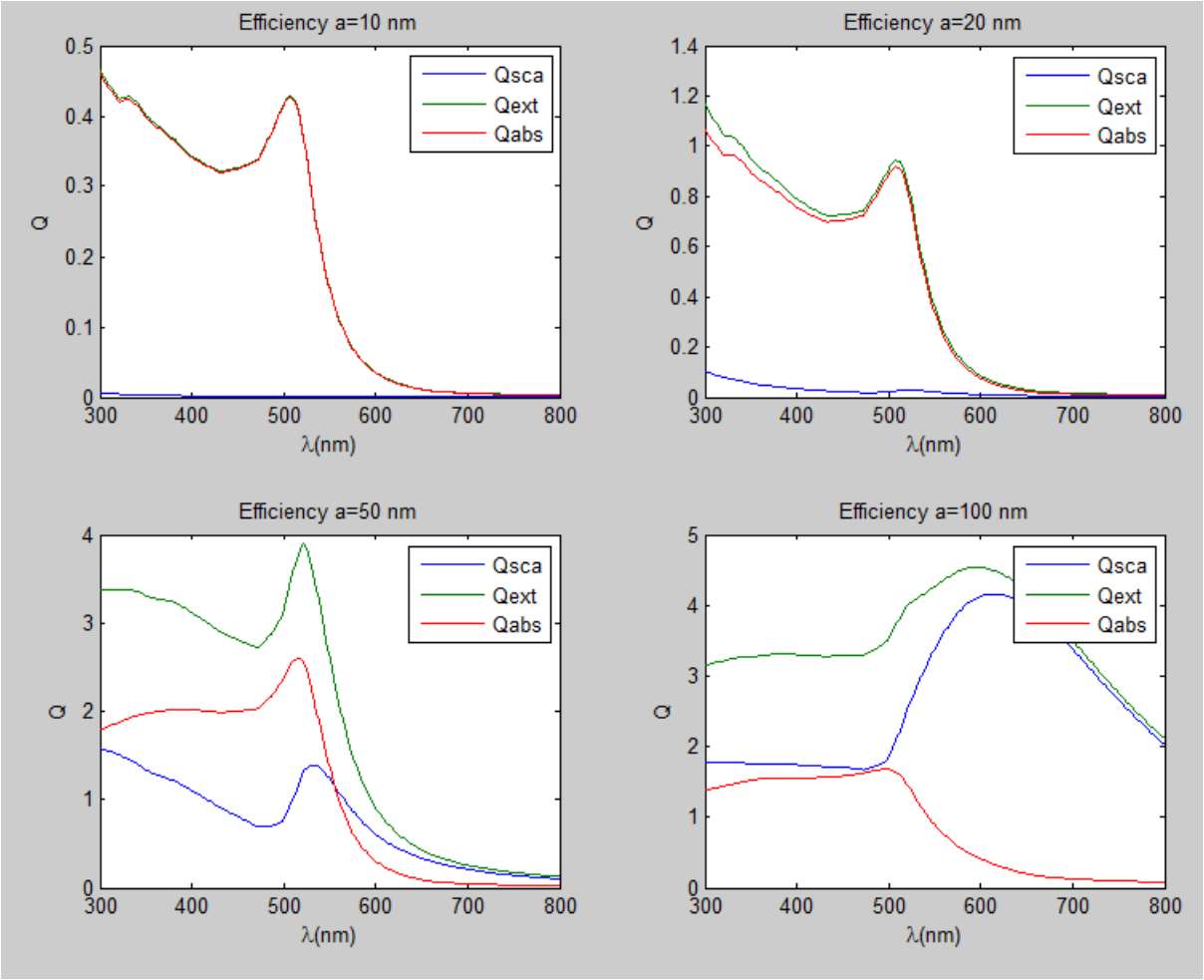

Figure 2.3: Efficiency against wavelength for a sphere radius of 10, 20, 50, *and* 100 *nm. There are shown three efficiencies, scattering in blue, extinction in green, and absorption in red.*

This comparison allows the reader to understand that absorption due to tiny spheres is very much larger than the scattering they produce , and how the scattering becomes more and more relevant as the sphere size increases.

It is also interesting to analyse how the cross section behaves as the radius of the sphere increases.

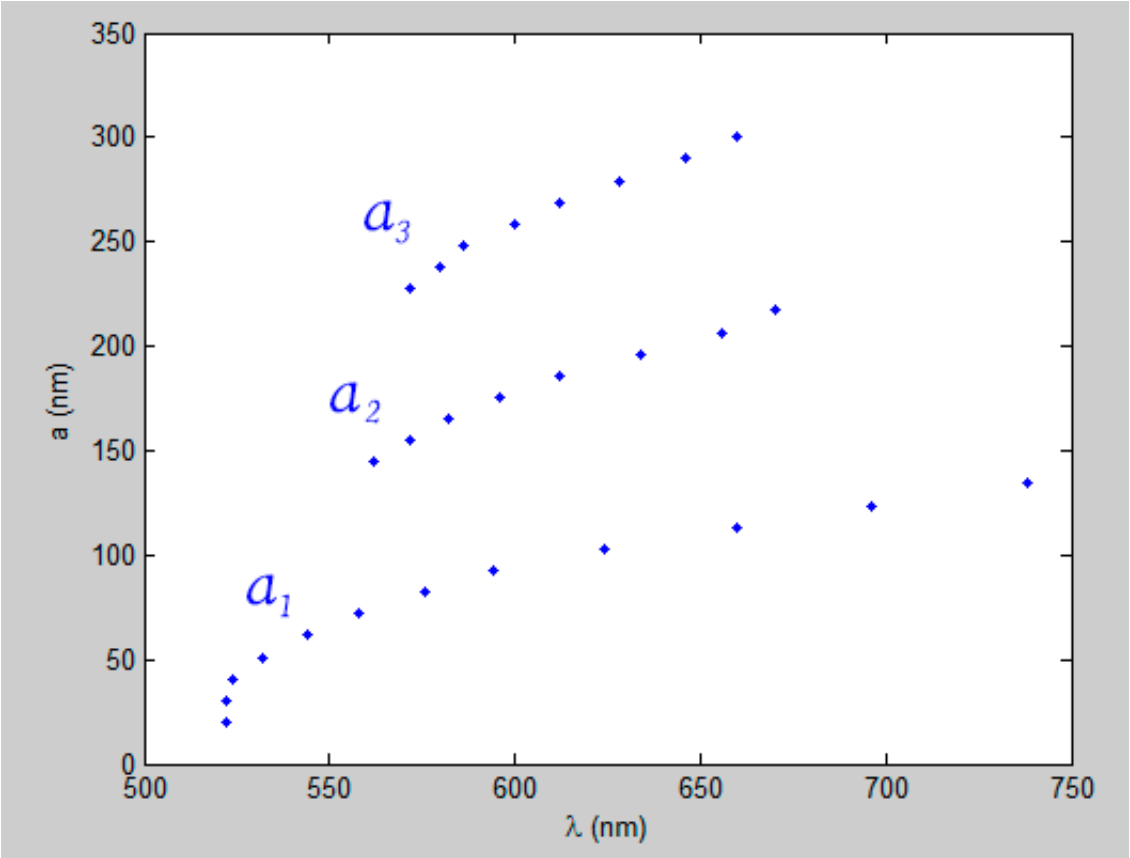

Figure 2.4: Wavelength at which the scattering cross section has a maximum for radius values from 20 *to* 300 *nm.*

For small radius values compared to the incident wavelength, the coefficient a_1 is the most relevant one, which is associated with the electrical dipole mode. As long as the radius of the sphere increases, it is seen that other terms begin to increase until they become relevant, which makes a shift in the maximum cross section. Thus, *Figure 2.4* proves that the peak of the spectrum suffers a redshift when the particle size increases, due to the evanescent waves that appear in the near field regime [27].

The *Figure 2.4* shows a kind of backward behaviour because the data of the first curve are only due to the first coefficient a_1, but the data of the second and the third curves correspond to the higher coefficients a_2 and a_3 respectively.

Hence, for particles larger than 100 or 150 nm, the cross section is dominated by higher order electron oscillations.

Chapter 3

Near field and dipole approximation

This chapter deals with the connection between electrostatics and scattering by small spherical particles compared with the wavelength. This is done by studying a pure dipole approximation, i.e. the nanoparticle is seen as a punctual dipole. This is a useful approximation either for very small particles (near to be punctual, so the nanoscale) and far field, being its range of validity studied in *Section 3.3.1*.

3.1. Far field vs near field

There are two regimes for which there are different kinds of scattering. Rayleigh scattering occurs when the particle size is less than 1/10 times the wavelength of the incident light. If the particle is bigger, with a size between $\lambda/10$ to λ, the scattering is known as Mie scattering, because it is well described by the Mie theory. As it can be seen in *Figure 3.1*, the scattered light direction is different for each kind of scattering, the scattering of light in the forward direction becomes more pronounced as the particle size increases.

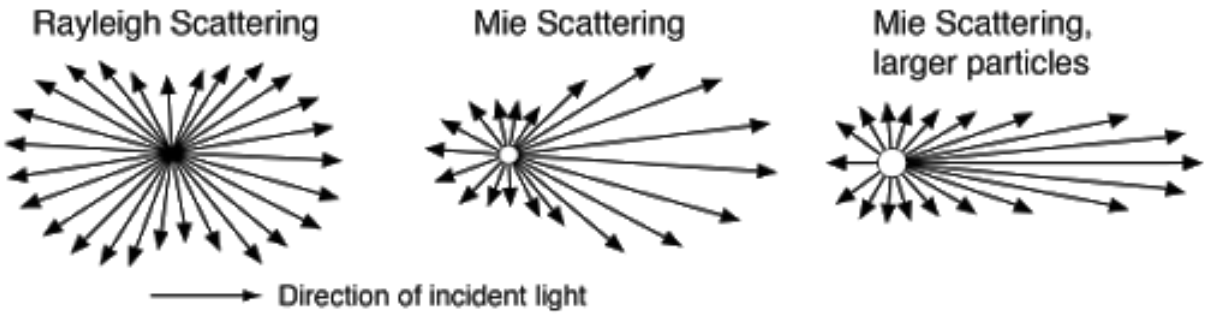

Figure 3.1: Scattering schemes according to the particle size [28].

As visible light goes from around 400 nm to 700 nm, Rayleigh scattering occurs for particle sizes lower than 50 nm in diameter; instead for Mie scattering, the particle sizes are between 50 nm and 500 nm, reaching optical scattering for larger particles.

Mie theory is able to describe the amplitude and phase of the fields scattered by a nanosphere, for either far or near fields since it uses summations of infinite terms. How-

ever, for small particles compared to the wavelength, some approximations can make the calculus easier.

Mie theory described in *Section 2.1* is the exact solution for any case, but for small particles compared with the wavelength, it can be simplified by using only dipolar contributions. Thus passing from Mie scattering to Rayleigh approximation by taking only the first scattering coefficient, obtaining the same result than the one obtaied by considering only an ideal dipole.

3.2. Dipole approximation

Light scattering and absorption by a nanoparticle can be considered as produced by electromagnetic radiation source [29]. The simplest radiator is an oscillating electric dipole with dipole moment **p** described in texts like reference [30] or [31].

A pure dipole is an ideal dipole, which means that there is no distance between positive and negative charges, rather, the source has no structure, is a point. Thus, approaching dipole as pure dipole can only be valid when the fields are calculated in a far field region and when the particle is really small.

Taking into account the display of the field of a linear electric dipole polarized in z direction, it is considered the general equations where p is the ideal dipole moment to obtain the equivalent field for a dipole polarized along the x direction (see *Section 3.3*):

$$\mathbf{E} = \left(\frac{3\,[p]}{r^5} + \frac{3\,[\dot{p}]}{cr^4} + \frac{3\,[\ddot{p}]}{c^2r^3}\right)(\mathbf{n}\cdot\mathbf{r})\cdot\mathbf{r} - \left(\frac{[p]}{r^3} + \frac{[\dot{p}]}{cr^2} + \frac{[\ddot{p}]}{c^2r}\right)\mathbf{n} \tag{3.1}$$

$$\mathbf{H} = \left(\frac{[\dot{p}]}{cr^3} + \frac{[\ddot{p}]}{c^2r^2}\right)(\mathbf{n}\times\mathbf{r}) \tag{3.2}$$

In *Eq* (3.1) and *Eq* (3.2) the vector **n** represents the direction of polarization and **r** the direction of propagation, c is the velocity of light in the medium (vacuum for this problem), and r is the radial vector, in spherical polar coordinates, which define the distance between the center of the particle and the point where the field is calculated. If n is a unitary vector along the x axis then *Eq* (3.3), *Eq* (3.4) and *Eq* (3.5) hold.

$$\mathbf{n} = \hat{x} = \sin\theta\cos\phi\ \ \hat{r} + \cos\theta\cos\phi\ \ \hat{\theta} - \sin\phi\ \ \hat{\phi} \tag{3.3}$$

$$\mathbf{r} = r\ \ \hat{r} \tag{3.4}$$

$$(\mathbf{n}\cdot\mathbf{r})\cdot\mathbf{r} = r^2\sin\theta\cos\phi\ \ \hat{r} \tag{3.5}$$

Replacing those vectors in *Eq* (3.1), it is obtained the field expression for each spherical polar coordinates.

$$\left.\begin{aligned} E_r &= 2\left(\tfrac{[p]}{r^3} + \tfrac{[\dot{p}]}{cr^2}\right)\sin\theta\cos\phi \\ E_\theta &= -\left(\tfrac{[p]}{r^3} + \tfrac{[\dot{p}]}{cr^2} + \tfrac{[\ddot{p}]}{c^2r}\right)\cos\theta\cos\phi \\ E_\phi &= \left(\tfrac{[p]}{r^3} + \tfrac{[\dot{p}]}{cr^2} + \tfrac{[\ddot{p}]}{c^2r}\right)\sin\phi \end{aligned}\right\} \tag{3.6}$$

$$\left.\begin{aligned} H_r &= 0 \\ H_\theta &= -\left(\frac{[\dot{p}]}{cr^2} + \frac{[\ddot{p}]}{c^2 r}\right)\sin\phi \\ H_\phi &= -\left(\frac{[\dot{p}]}{cr^2} + \frac{[\ddot{p}]}{c^2 r}\right)\cos\theta\cos\phi \end{aligned}\right\} \tag{3.7}$$

Those equations describe the field in every point of the space, they completely describe the near field, but for the far field they can be approximated by

$$\left.\begin{aligned} E_\theta &= -\frac{[\ddot{p}]}{c^2 r}\cos\theta\cos\phi \\ E_\phi &= \frac{[\ddot{p}]}{c^2 r}\sin\phi \end{aligned}\right\} \tag{3.8}$$

$$\left.\begin{aligned} H_\theta &= -\frac{[\ddot{p}]}{c^2 r}\sin\phi \\ H_\phi &= \frac{[\ddot{p}]}{c^2 r}\cos\theta\cos\phi \end{aligned}\right\} \tag{3.9}$$

where radial components are neglected at great distances because they decrease faster as the distances increase.

Looking at the $x - z$ plane, that means $\phi = 0$, and through equations *Eq* (3.6) for near field and *Eq* (3.8) for a far field, it is evident that the maximum value of the electric field in the near field case, will be in the x direction, and in the far field case the maximum will appear perpendicular to the x direction.

In *Figure 3.2* can be seen that for a dipole polarized in x direction, in the near field regime (top left) the maximum field intensity will be found in the x direction, but in the far field regime (top right) it will radiate in the perpendicular direction.

The plots in *Figure 3.2* were generated with the MatLab software using *Eq* (3.6) and *Eq* (3.8) to calculate them

As the ideal dipole is a point in the origin of coordinates, it cannot be represented, nevertheless, in order to facilitate the visualization of the direction of the electric field, this was only calculated starting at a distance r form the dipole, represented by the dark blue circle of the figures. The figure at the top right and the figure bottom represent the same case: far field. But in the bottom figure, the near field representation is suppressed by calculating the field only for large values of r, making the dark blue circle bigger.

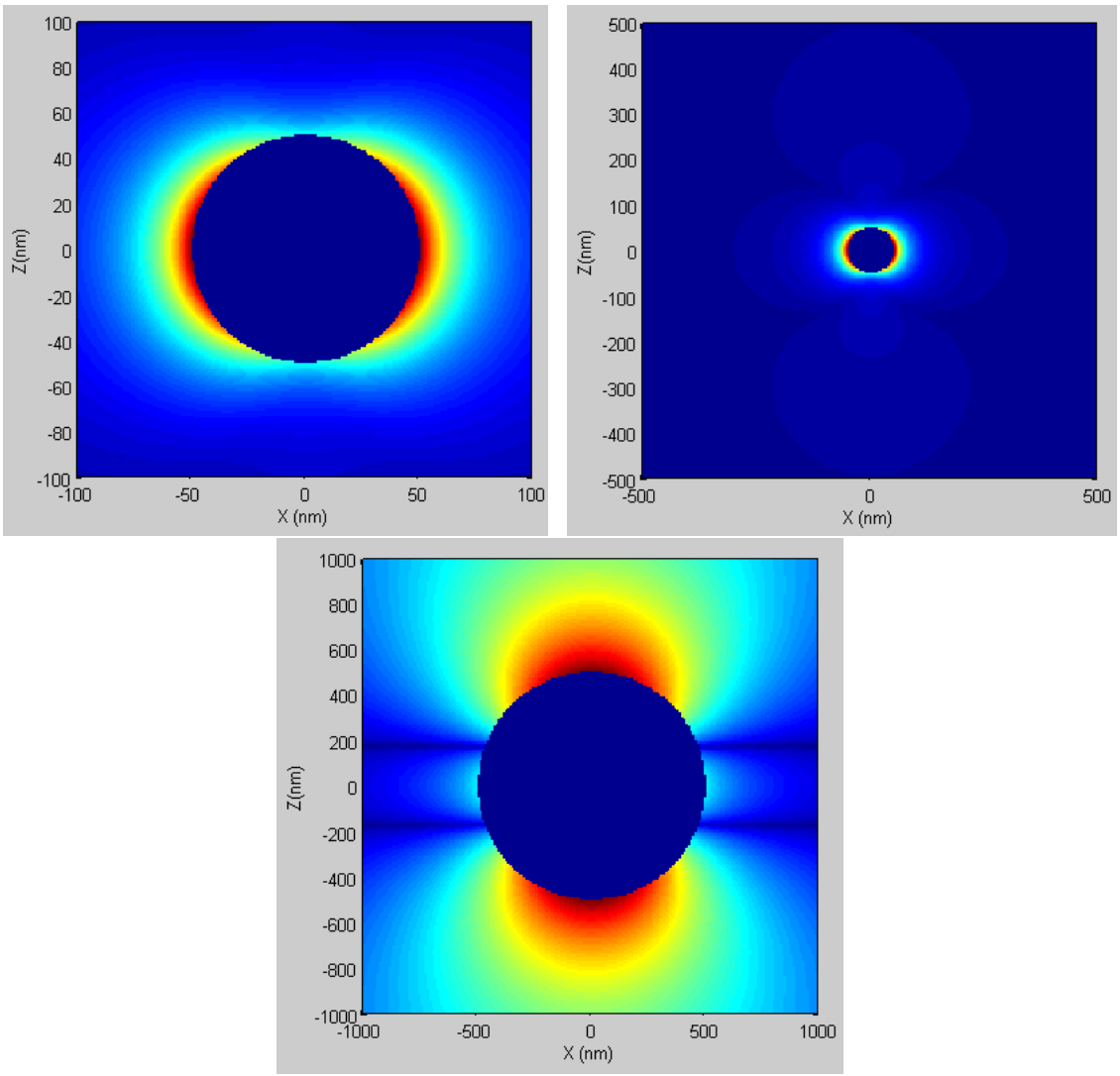

Figure 3.2: Dipole scattering electric field calculated for a distance from the surface of the sphere between 50 *nm and* 100 *nm (top left), from* 50 *nm to* 500 *nm (top right), and from* 500 *nm to* 1000 *nm (bottom), to compare the predominant direction of the field in near(top left) and far field (top right and bottom). The color code corresponds to the intensity of the scattered electric field, where red corresponds to the greatest values while dark blue is close to the null intensity.*

3.3. Electrostatic approximation

The electrostatic approximation takes place when the field variations are negligible, so this approximation describes the response of an sphere to an applied uniform static field. If the region of the space considered is delimited by a sphere which size is much smaller than the wavelength of the field, then the situation is equivalent to the case of a sphere immersed in a uniform field.

As permittivities of the sphere and the medium are different, a charge will be induced on

the surface of the sphere, so the field outside the sphere is derivable from the potential Φ.

$$\mathbf{E} = -\nabla \mathbf{\Phi} \tag{3.10}$$

As a dipole is defined as two opposite charges, the ideal dipole is obtained getting the charges closer to one another. The ideal dipole potential is define by:

$$\mathbf{\Phi} = \frac{\mathbf{p} \cdot \mathbf{r}}{4\pi\varepsilon_m a^3} \tag{3.11}$$

where ε_m is the permitivitty of the medium and a is the radius of the sphere.

The field outside the sphere is the superposition of applied field and the field of an ideal dipole with moment:

$$\mathbf{p} = 4\pi\varepsilon_m a^3 \frac{\varepsilon_1 - \varepsilon_m}{\varepsilon_1 + 2\varepsilon_m} \mathbf{E_0} \tag{3.12}$$

where ε_1 is the permitivitty of the sphere, E_0 is the amplitude of the wave and α is the polarizability of the nanosphere, defined as:

$$\alpha = 4\pi a^3 \frac{\varepsilon_1 - \varepsilon_m}{\varepsilon_1 + 2\varepsilon_m} \tag{3.13}$$

The polarizability is a measure of how strong a particle scatters and absorbs light, and how the incident field is enhanced in the vicinity of the particle. As it can be seen in *Eq* (3.13), the polarizability depends on the particle size a and its permitivitty ε_1.

Regarding small spheres, there is a resonance when the denominator of *Eq* (3.13) becomes zero, which is $\varepsilon_1 = -2 \cdot \varepsilon_m$. The frequency at which resonance takes place is named Fröhlich mode, and if the object is metallic this resonance is known as plasmon resonance, which amplitude reaches the maximum for a specific frequency. Hence, plasmon resonance is determined by the polarizability (α) and plasma frequency (ω_p) [32].

The plasma frequency is defined by

$$w_p = \sqrt{\frac{e^2 \cdot n}{m_e \cdot \varepsilon_0}} \tag{3.14}$$

and the resonance frequency in spheres is

$$w_{res} = \frac{w_p}{\sqrt{3}} \tag{3.15}$$

Consequently, considering a free electron density around $n = 10^{28}\ electrons/m^3$, the charge of the electron is $e = 1.6 \cdot 10^{-19}\ C$, the mass of the electron is $m_e = 9.1 \cdot 10^{-31}\ kg$, and the permittivity of vacuum $\varepsilon_0 = 8.85 \cdot 10^{-12}\ F/m$, the resonance frequency of gold is contained in the range ultraviolet-visible. In this problem, the surrounding medium is vacuum, but for other mediums it is important to remind that the permittivity is a wavelength dependant value.

Conduction electrons of the sphere react to the external field by producing a net positive charge on one side of the particle, and a net negative charge on the other, see *Figure 3.3*. The displacement of negative and positive charges induces the dipole which strength depends

on the polarization. The resonance is on account of Coulomb force, which determines the frequency of resonance by the restoring force of the displaced charges.

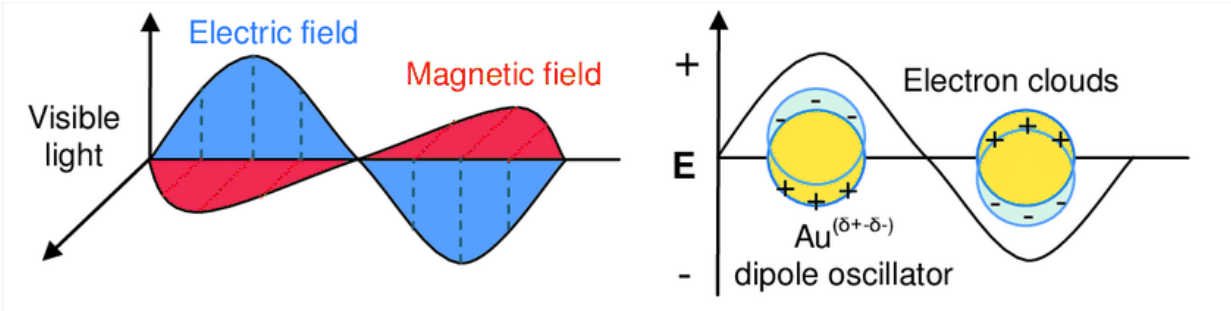

Figure 3.3: The scheme of the electromagnetic field of visible light and its interaction with gold nanoparticles. Oscillating dipoles induced by electromagnetic radiation [33].

The real part of the dielectric constant of the metal determines the surface plasmon resonance position and the imaginary part determines the bandwidth.

Figure 3.2 can be compared with the equivalent one for this approximation, *Figure 3.4*, confirming that the shape of the electric field is the same in both cases. However, in *Figure 3.4*, the dark blue circle represents the gold nanosphere of 50 *nm* of radius, that is why here it is not shown the third plot, because the blue circle of 500 *nm* would represent a gold sphere with a radius of 500 *nm*.

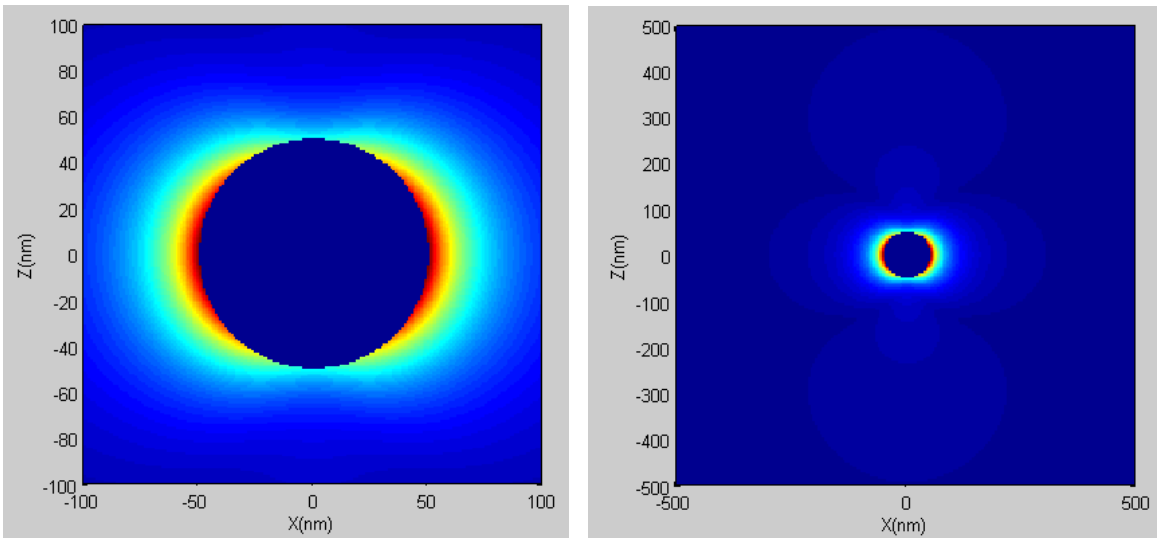

Figure 3.4: Scattering electric field calculated with the electrostatic approximation for a distance from 50 nm to 100 nm (left) representing the near field, and from 50 nm to 500 nm (right) representing the far field. The color code corresponds to the intensity of the scattered electric field, where red corresponds to the greatest values while dark blue is close to the null intensity.

3.3.1. Range of validity

Looking at the polarizability expression *Eq* (3.13), it can be seen that when the size of the particle increases, the polarizability increases as well.

Considering what has been exposed in *Figure 2.4*, and knowing that the term a_1 is the one related with the electric dipole mode, the dipole approximation will be valid until the second term is comparable to the first one.

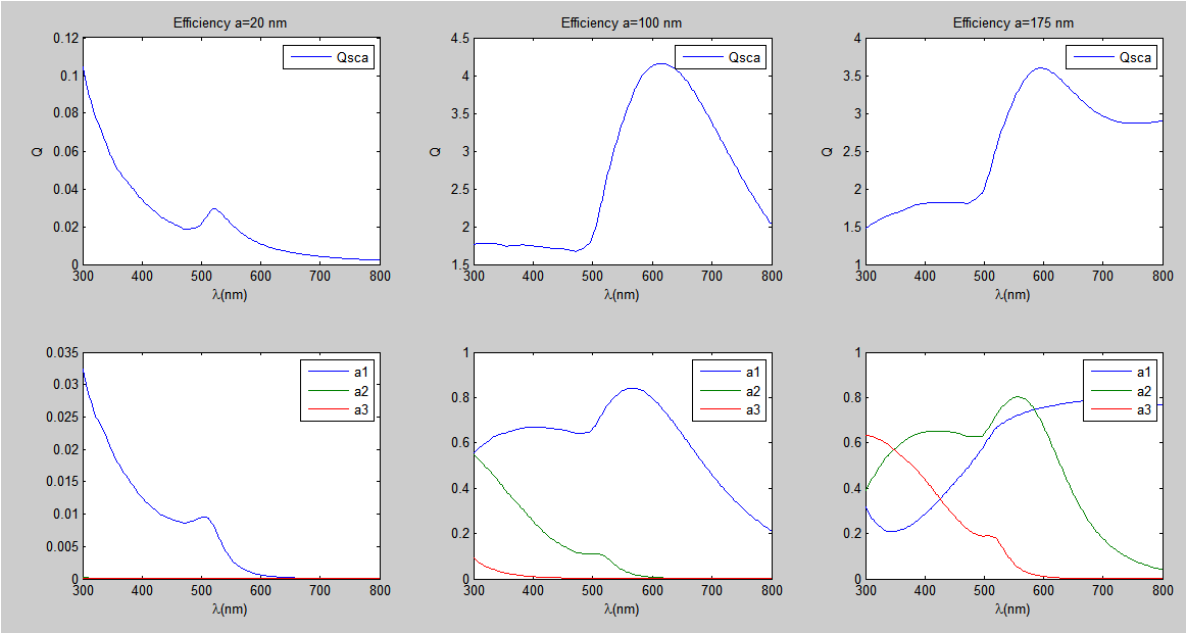

Figure 3.5: Efficiency in a wavelength range from 300 *to* 800 *nm, for a gold sphere of* 20, 100 *and* 175 *nm of radius. Below each one,* a_n *coefficients are represented to appreciate their influence.*

In *Figure 3.5*, it can be seen that for a radius of 20 *nm* only the first term influences the scattering efficiency. While the radius grows, other terms appear, even being larger than the first one as in the 175 *nm* case. Hence, the range in which the dipole approximation is valid could be expressed as nanoscale, or radius below 100 *nm*.

Electric field analysis

Once the range of validity of dipole approximation is known, it is time to depict and compare the Mie theory electric field with a pure dipole electric field.

To visualize this comparison, in *Figure 3.6* and *Figure 3.7* the modules of the scattering electric field cartesian components are represented, as well as the module of the total scattering electric field by a gold nanosphere of radius 20 *nm* when it is illuminated by a plane electromagnetic wave of 550 *nm* of wavelength.

Figure 3.6 and *Figure 3.7* concur with the range of validity, showing that for a gold nanosphere with radius $a = 20\ nm$ surrounded by vacuum and illuminated by an electromagnetic wave polarized in x direction with $\lambda = 550\ nm$, the Mie scattering field is the same than the pure dipole field for each component and for the total field too.

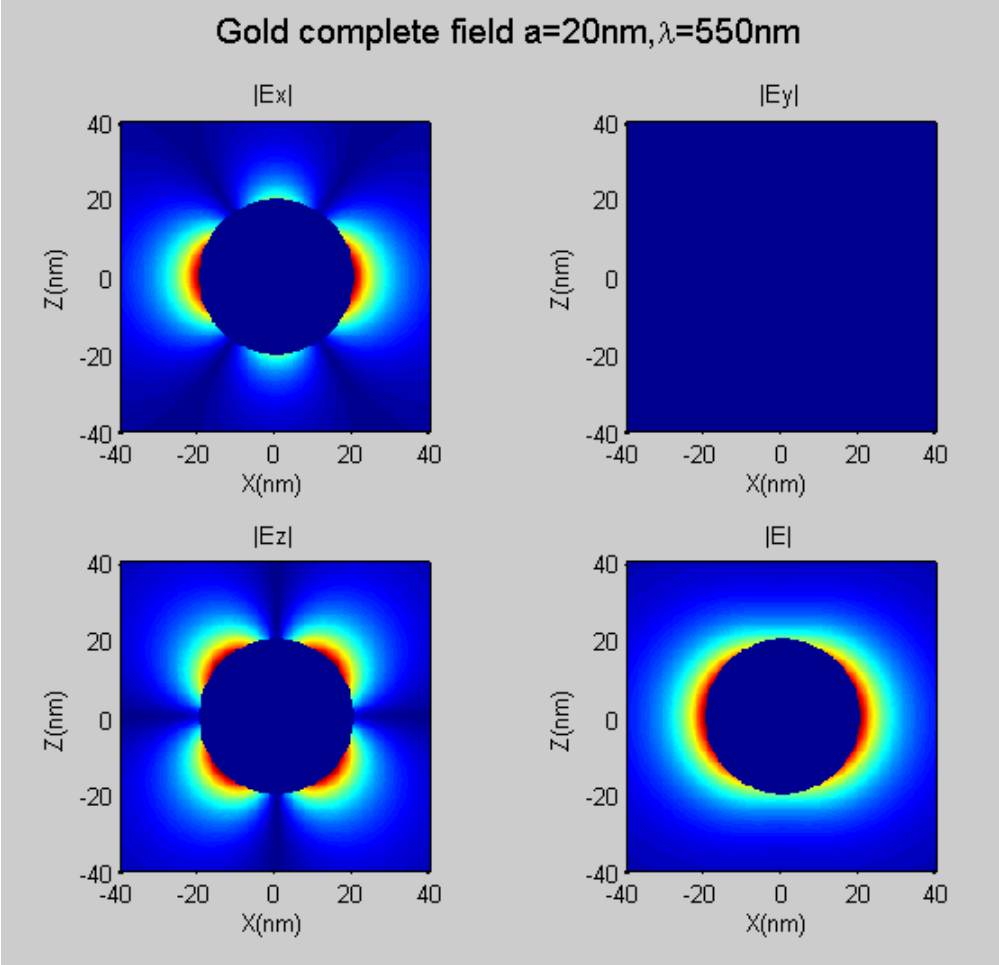

Figure 3.6: Scattered electric field by a gold nanosphere with a radius of 20 *nm, calculated by Mie Theory (in this case it has been used the first 5 terms of Eq* (2.11)*). Each figure represents the module of the cartesian coordinate x, y or z, being above on the left, above on the right and below on the left respectively; and below on the right is the module of the total scattered field. The color code corresponds to the intensity of the scattered electric field, where red corresponds to the greatest values while dark blue is close to the null intensity.*

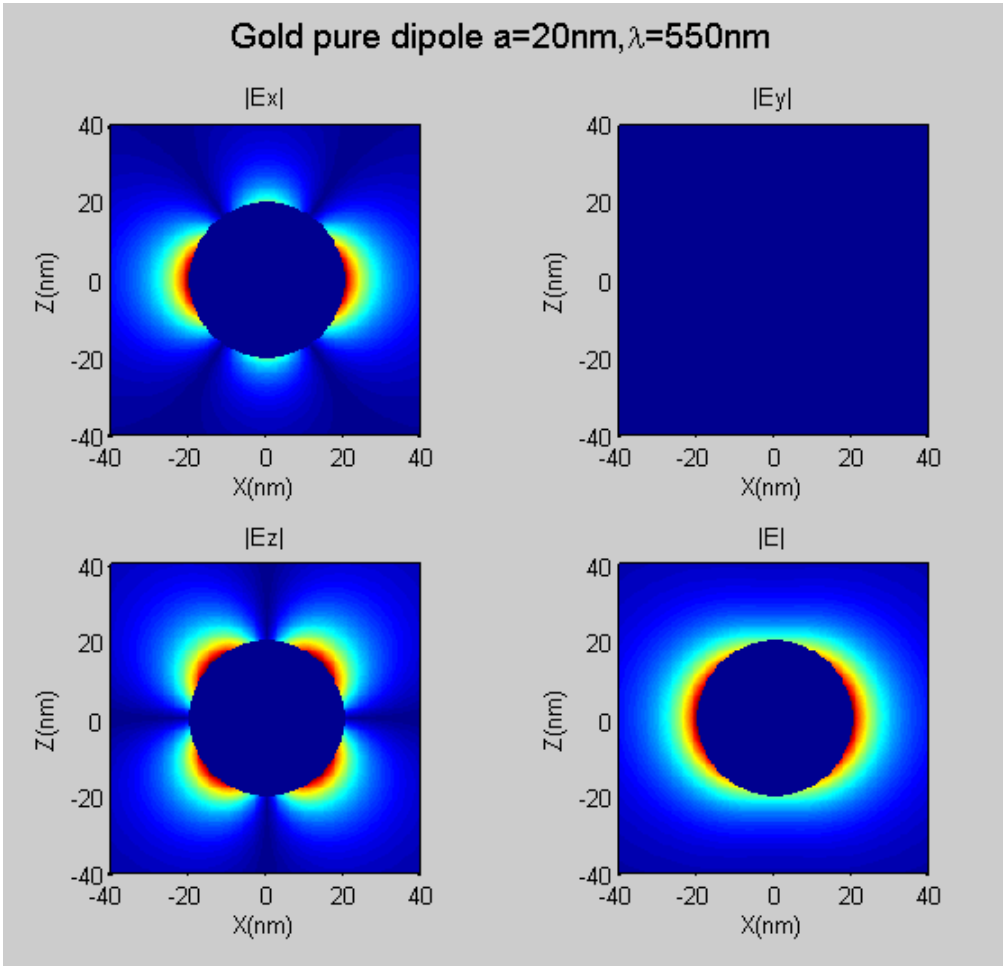

Figure 3.7: Scattered electric field by a gold nanosphere with a radius of 20 *nm, calculated with the dipole approximation (using Eq* (3.6)*). The plot distribution is the same as in Figure 3.6. The color code corresponds to the intensity of the scattered electric field, where red corresponds to the greatest values while dark blue is close to the null intensity.*

Chapter 4

Near electric field and Poynting vector

This chapter goes over the change of polarization definition for different fields ranges. Besides, the relationship between the electric field and the flux of energy is discussed.

Focusing the analysis on the near field regime, the electric field and the Poynting vector are used to get insight into the evanescent waves on the sphere surface, which are non propagating and inhomogeneous waves.

4.1. Gold nanosphere near electric field

When the sphere is smaller than the wavelength, only the first electric mode needs to be taken into account to describe the scattered field, as it has been explained in *Section 3.3*. In the case of gold, the maximum intensity of the field is found at wavelength between 500 and 600 nm depending on the particle size; this maximum is related to a resonance in the electrons displacement.

The plot in *Figure 4.1* represents the electric field scattered by a gold nanoparticle of 20 nm surrounded by vacuum and illuminated by a plane wave of $\lambda = 550\ nm$, obtained with *Eq* (3.6). The intensity of the electric field is represented in a grayscale is represented the intensity of the electric field, and the blue arrows represent the electric field vector in the $x-z$ plane.

The obtained result corresponds to the scattered electric field in the near field regime, which is the same for the full field Mie theory, dipole approximation and electrostatic approximation calculus, as it has been seen in Chapter *3*.

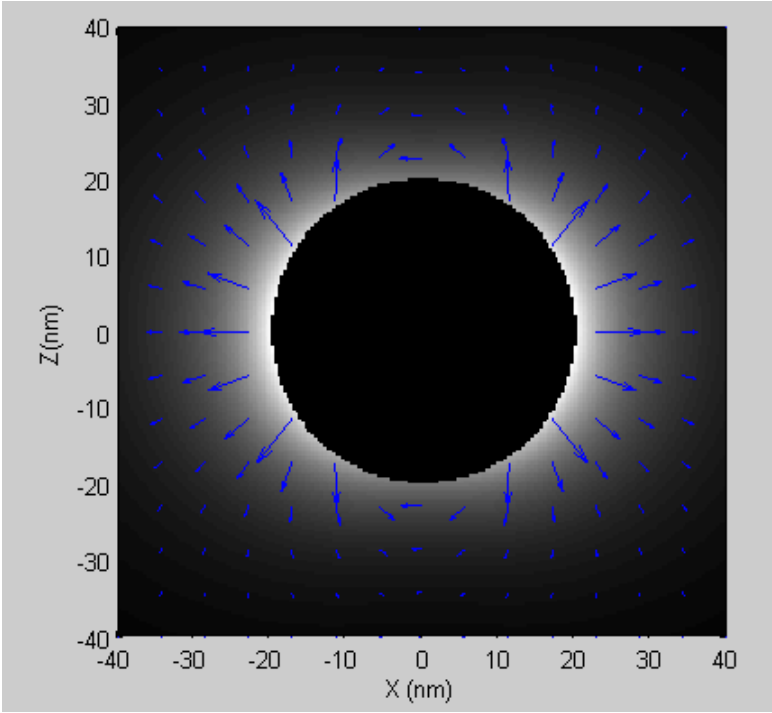

Figure 4.1: Scattering electric field into near field approximation for a gold nanosphere of radius 20 *nm.*

4.2. Gold nanosphere near field Poynting vector

Poynting vector is a magnitude of that describes how much energy per second flows per square meter. In this case, we are interested in the time average Poynting vector which can be written as:

$$\mathbf{S} = \frac{1}{2} \cdot Re\{\mathbf{E} \times \mathbf{H}^*\} \tag{4.1}$$

where $\mathbf{S}$ represents the Poynting vector, $\mathbf{E}$ the electric field vector, and $\mathbf{H}$ the magnetic field vector. The asterisk $(*)$ over the magnetic field vector means the conjugate vector, and Re is for the real part of its content.

Figure 4.2 display the real part of the electric field (in blue), the real part of the magnetic field (in red), and the Poynting vector (in green) in three dimensions. Above is the electrostatic approximation with the yellow sphere representing the gold nanosphere; and below is the dipole approximation case.

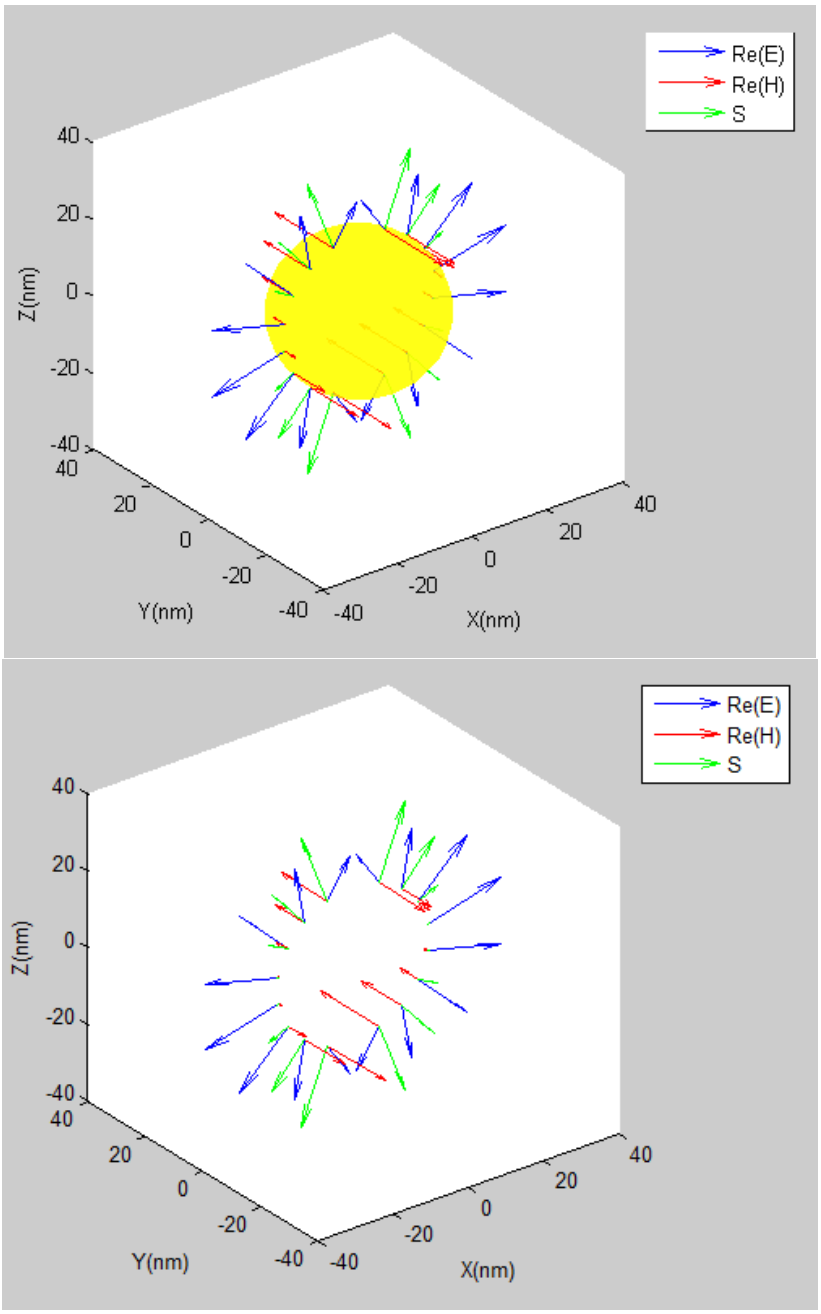

Figure 4.2: Electric and magnetic field, and Poynting vector calculated with electrostatics approximation (above) and dipole approximation (below).

As can be seen, Poynting vector is determined by the electric and magnetic fields. Electric and magnetic fields are in phase and perpendicular between them, and both are perpendicular to the direction of propagation, so Poynting vector will be in the direction of propagation as well because of the cross product in *Eq* (4.1).

Despite this, in the near field case, the electric field does not have to be completely perpendicular to the Poynting vector (see *Figure 4.3*), this is due to the polarization definition explained in *Section 4.3*.

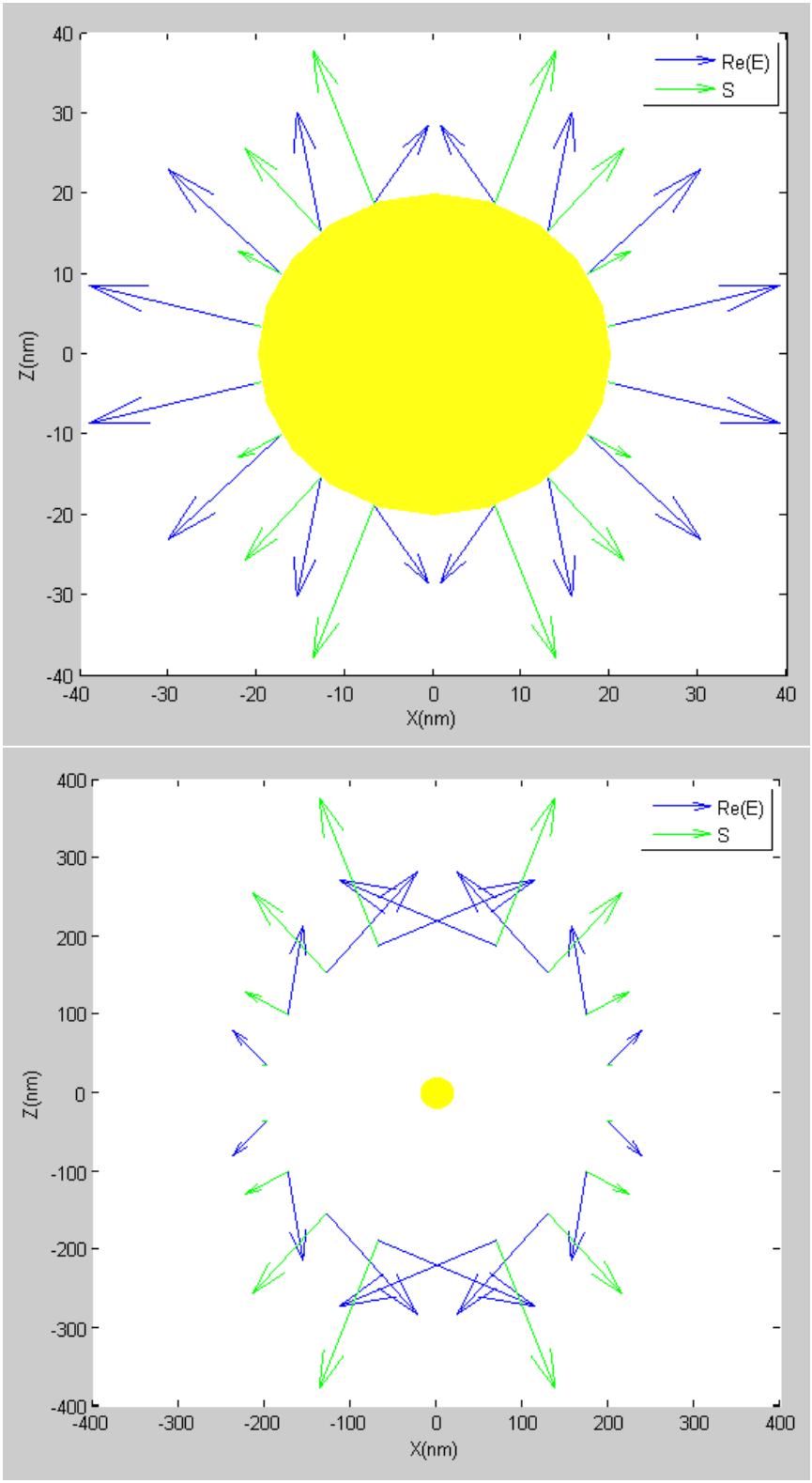

Figure 4.3: Scattered electric field and Poynting vector at a distance of 20 *nm (top) and* 200 *nm (botttom). The yellow circle represents a gold nanosphere with a radius equal to* 20 *nm in both cases.*

In general, electric and magnetic fields are perpendicular to the Poynting vector, however, in the near field region they are not perpendicular to **S**. This is because, in the vicinity of a metallic surface, the near field region, there is a non-propagating field associated to evanescent waves.

When *Eq* (4.2) is satisfied, **S** and $Re\mathbf{E}$ are perpendicular, and when it is equal to zero means that they are parallel. This allows the distinction between common electric field and evanescent waves.

$$\mathbf{S} \times Re\{\mathbf{E}\} \cdot \frac{\mathbf{S} \cdot Re\{\mathbf{E}\}}{|\mathbf{S} \cdot Re\{\mathbf{E}\}|} = 1 \tag{4.2}$$

4.3. Gold nanosphere near field degree of polarization

The polarization is the property that describes the geometrical orientation of electric field oscillations. All over this work, it has been used as a source of light linearly polarized; that means it is a transverse wave where electric and magnetic fields are coupled and they are perpendicular to each other, oscillating in a single direction, and they are also perpendicular to the direction of propagation.

There is also important to point out that there are waves where oscillations are not limited by perpendicular directions to the propagation way.

Polarization in far field can be explained by a two-dimensional plane where are contained the electric and magnetic field, as it has been seen before and in *Figure 1.5*. In this case, the scattered electric field is purely transverse to the radial component as can be deduced from *Eq* (3.8) and seen in *Figure 4.4*.

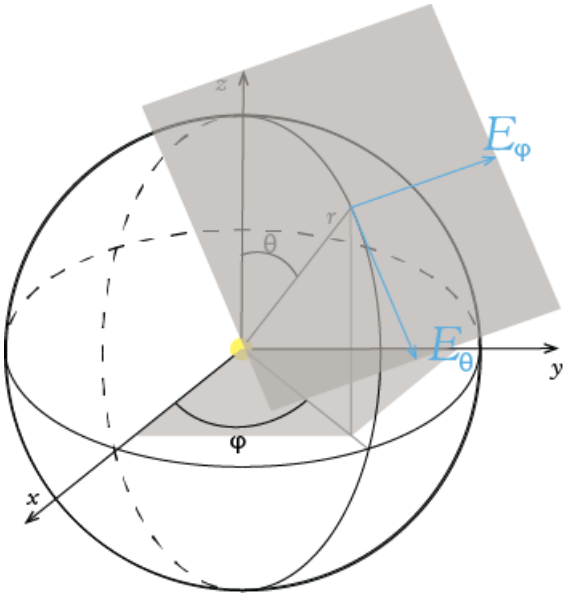

Figure 4.4: Components of electric scattered field in spherical polar coordinates in the far field regime.

Nevertheless, the near field is not contained in the perpendicular plane to the radial direction, because near field is three-dimensional, see *Eq* (3.6) or *Figure 4.5*. The physical interpretation is that non-propagating waves appeared in the near field, making different the explanation of the polarization at this range [34].

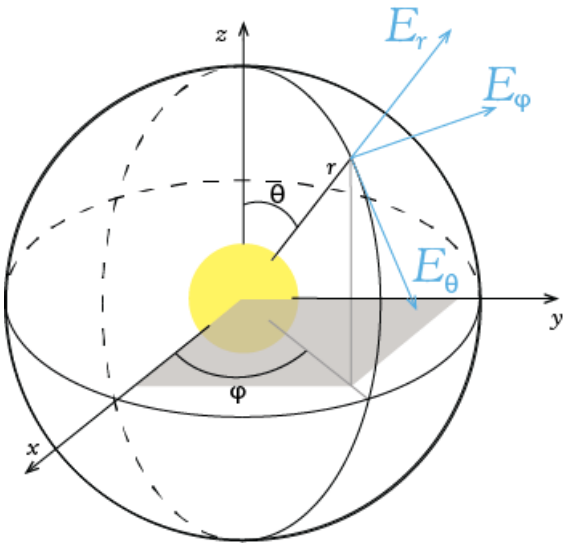

Figure 4.5: Components of electric scattered field in spherical polar coordinates in the near field regime.

By analysing the relation between the electric field and the Poynting vector, the amplitude of the electric field associated to the evanescent waves on the surface of a gold nanosphere can be represented taking the real part of the electric field and removing the field values that are perpendicular to the Poynting vector, the remaining field is not perpendicular to S, it means that the remaining field id the field associated to the evanescent waves, which is represented in *Figure 4.6*. Where the calculus of left plot is given by *Eq* (3.6) and the right one by the subtraction of *Eq* (3.6) minus *Eq* (4.2).

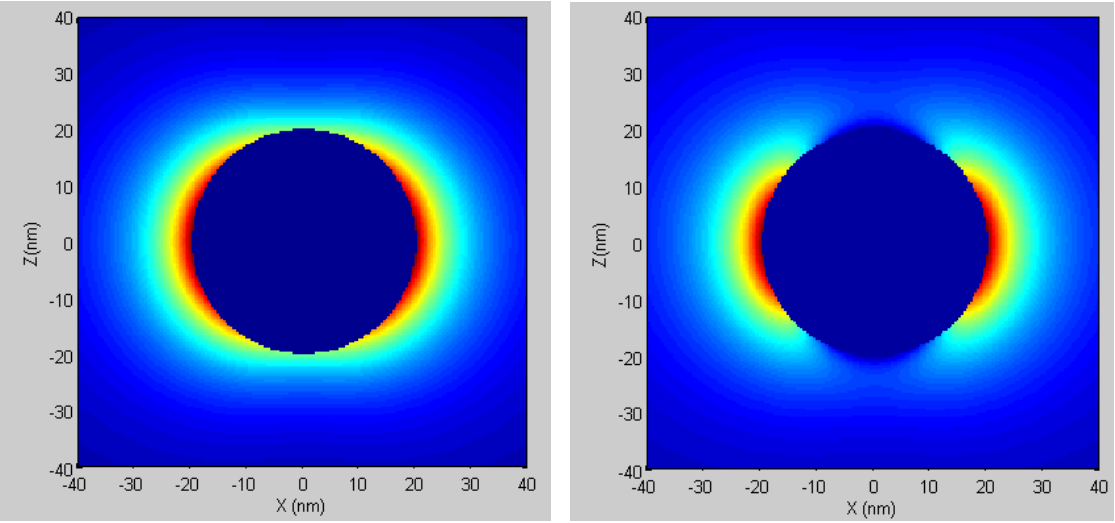

Figure 4.6: Enhanced scattered electric field of a gold nanosphere of a radius of 20 *nm (left). Amplitude of the electric field associated to evanescent waves on the surface of a gold nanosphere of a radius of* 20 *nm (right). The color code corresponds to the intensity of the scattered electric field, where red corresponds to the greatest values while dark blue is close to the null intensity.*

In *Figure 4.6* can be appreciated two regions where there is a field enhancement, known as "hot spots", which are relevant in many applications mentioned in Chapter *1* such as cancer cell detection.

Hot spots can be found where the amplitude and confinement of the evanescent field reaches its maximum, becoming an interesting branch of study due to its possible applications [15].

As mentioned in the introduction (Chapter *1*), the oscillations of the electrons confined to the surface of the metallic nanostructures are known as localised surface plasmon resonances (LSPRs). They decay radiatively via photon emission, or non radiatively through the generation of excited carriers in the regions known as hot spots [35]. In addition, surface plasmons can couple to electromagnetic fields emitted by other molecules or quantum dots placed in the nanoparticle proximity [4].

Thus, the energy is compressed into subwavelength scale via keeping part of it as kinetic energy of conduction electrons. Using localised surface plasmon resonances lead to an extreme location of the electric field on the nanoscale, making it into efficient optical nanoantennas [36]. Furthermore, the enhancement of the electric field is stronger between two metal nanoparticles, near to each other, rather than a single one [37].

Actually there is currently a great interest in the use of hot spots due to LSPRs for the detection of enantiomers in a very sensitive way. Enantiomers are chiral molecules that are mirror images of each other and they are not superposable, which may not have identical physicochemical properties even if they have exactly the same atomic composition. They are often identified by optical methods because they usually exhibit optical activity, it means that they tend to change the state of polarization of polarized light.

Chapter 5

Conclusions and future work

In this research, it has been studied the field scattered by a metallic nanosphere illuminated by a plane electromagnetic wave to understand the behaviour of electromagnetism in the vicinity of the particle and their unique optical properties.

After justifying the characteristics of the chosen problem, the objectives have been reached with the aid of the code shown in Appendix *A*. The code enables to calculate the scattered electric and magnetic fields, with which it has been obtained the vector of the flux of energy.

The material, shape, size, composition, and dielectric constant of the particle and the surrounding medium are the parameters to keep in mind to design a nanoscale experiment or application based in light scattering.

On one hand, larger nanoparticles are usually chosen for imaging applications due to their larger scattering efficiency. On the other hand, small nanoparticles are preferred to convert the energy carried by light into thermal radiation because of their larger light absorption efficiency; it is useful for killing cells or burning tissues in biomedical applications.

In the near field regime there have been found exceptional properties due to the optical response of a metallic surface when it interacts with a plane electromagnetic wave plane. It is relevant to mention that these properties depends on different parameters such as surface size, shape and morphology, characteristics that can be modified by temperature, pressure time and pH conditions. Near field analysis provides another line of work related to non-propagating waves, named as plasmonics.

Polarization also plays an important role in defining some properties related to chirality. Polarization has not a fixed definition, as it has been discussed, it is crucial to consider the specific conditions of each case, bringing the degree of polarization concept to the polarization concept.

Localised surface plasmon resonances produce enhancements of the electromagnetic field in the near field of metallic nanostructures. Thanks to surface plasmon resonances, the absorbed and scattered light may be enhanced in 5 or 6 orders of magnitude compared to the strongly absorbing dye molecules and the emission of strongly fluorescent molecules. The study of surface plasmon resonances implies to consider both the radiative and non radiative properties of the emitter, and thus, the use and possible applications of those emitters.

Plasmon-induced phenomena are attracting an increasing research interest due to their potential for applications in photocatalysis, photodetection, and solar energy harvesting. Making it a very promising field for oncoming investigations.

Bibliography

[1] J. M. Sanz, D. Ortiz, R. Alcaraz de la Osa, J. M. Saiz, F. González, A. S. Brown, M. Losurdo, H. O. Everitt, and F. Moreno. Uv plasmonic behavior of various metal nanoparticles in the near- and far-field regimes: Geometry and substrate effects. *The Journal of Physical Chemistry C*, 117(38):19606–19615, Sep 2013.

[2] National Research Council. *Small Wonders, Endless Frontiers: A Review of the National Nanotechnology Initiative*.

[3] Suryani Saallah and Wuled Lenggoro. Nanoparticles carrying biological molecules: Recent advances and applications. *KONA Powder and Particle Journal*, 2018, 01 2018.

[4] Vincenzo Giannini, Antonio I. Fernández-Domínguez, Susannah C. Heck, and Stefan A. Maier. Plasmonic nanoantennas: Fundamentals and their use in controlling the radiative properties of nanoemitters. *Chemical Reviews*, 111(6):3888–3912, Jun 2011.

[5] David Pines. Collective energy losses in solids. *Rev. Mod. Phys.*, 28:184–198, Jul 1956.

[6] A. E. Rider, K. Ostrikov, and S. A. Furman. Plasmas meet plasmonics. Everything old is new again. *European Physical Journal D*, 66(9):226, September 2012.

[7] `http://www.evanescentoptics.com/technical-info/?id=4`. (Last visited 08/09/20).

[8] W. H. Weber and G. W. Ford. Optical electric-field enhancement at a metal surface arising from surface-plasmon excitation. *Opt. Lett.*, 6(3):122–124, Mar 1981.

[9] Christopher Green and Alun Vaughan. Nanodielectrics - how much do we really understand? [feature article]. *Electrical Insulation Magazine, IEEE*, 24:6 – 16, 08 2008.

[10] Ryan Tweney. Discovering discovery: How faraday found the first metallic colloid. *Perspectives on Science*, 14:97–121, 03 2006.

[11] Mark I. Stockman. Nanoplasmonics: past, present, and glimpse into future. *Opt. Express*, 19(22):22029–22106, Oct 2011.

[12] Martin Neugebauer, Peter Banzer, and Sergey Nechayev. Emission of circularly polarized light by a linear dipole. *Science Advances*, 5(6), 2019.

[13] Fang Pu, Yanyan Huang, Zhiguang Yang, Hao Qiu, and Jinsong Ren. Nucleotide-based assemblies for green synthesis of silver nanoparticles with controlled localized surface plasmon resonances and their applications. *ACS Applied Materials & Interfaces*, 10(12):9929–9937, Mar 2018.

[14] Xiaohua Huang and Mostafa A. El-Sayed. Gold nanoparticles: Optical properties and implementations in cancer diagnosis and photothermal therapy. *Journal of Advanced Research*, 1(1):13 – 28, 2010.

[15] F. Fornel. *Evanescent Waves: From Newtonian Optics to Atomic Optics*. 01 2001.

[16] Matthew E. Stewart, Christopher R. Anderton, Lucas B. Thompson, Joana Maria, Stephen K. Gray, John A. Rogers, and Ralph G. Nuzzo. Nanostructured plasmonic sensors. *Chemical Reviews*, 108(2):494–521, Feb 2008.

[17] David G Myszka. Kinetic analysis of macromolecular interactions using surface plasmon resonance biosensors. *Current Opinion in Biotechnology*, 8(1):50 – 57, 1997.

[18] Christian Kuppe, Kristina R. Rusimova, Lukas Ohnoutek, Dimitar Slavov, and Ventsislav K. Valev. "hot" in plasmonics: Temperature-related concepts and applications of metal nanostructures. *Advanced Optical Materials*, 8(1):1901166, 2020.

[19] Cyril Muehlethaler, Marco Leona, and John R. Lombardi. Review of surface enhanced raman scattering applications in forensic science. *Analytical Chemistry*, 88(1):152–169, Jan 2016.

[20] Harry Atwater and Albert Polman. Plasmonics for improved photovoltaic devices. *Nature materials*, 9:865, 10 2010.

[21] Jie Liang, Haizhou Liu, Jianyu Yu, Lin Zhou, and Jia Zhu. Plasmon-enhanced solar vapor generation. *Nanophotonics*, 8(5):771 – 786, 2019.

[22] Ibrahim Khan, Khalid Saeed, and Idrees Khan. Nanoparticles: Properties, applications and toxicities. *Arabian Journal of Chemistry*, 12(7):908 – 931, 2019.

[23] C. Bohren and D. R. Huffman. *Absorption and Scattering of Light by Small Particles*. Wiley Science Paperback Series, 1998.

[24] `https://refractiveindex.info/?shelf=main&book=Au&page=Johnson`. (Last visited 30/07/2020).

[25] Julius Adams Stratton. *Electromagnetic theory*. International series in pure and applied physics. McGraw-Hill, New York, NY, 1941.

[26] Gustav Mie. Beiträge zur Optik trüber Medien, speziell kolloidaler Metallösungen. *Annalen der Physik*, 330(3):377–445, January 1908.

[27] Fernando Moreno, Pablo Albella, and Manuel Nieto-Vesperinas. Spectral behavior of localized plasmon resonances in the near- and far-field regimes. comment on the spectral shift between near- and far-field resonances of optical nano-antennas, 2014. (arXiv:1407.4203).

[28] `http://hyperphysics.phy-astr.gsu.edu/hbase/atmos/blusky.html`. (Last visited 30/08/2020).

[29] Dr. Michael Quinten. *Mie's Theory for Single Spherical Particles*, chapter 5, pages 75–122. John Wiley Sons, Ltd, 2011.

[30] Max Born, Emil Wolf, A. B. Bhatia, P. C. Clemmow, D. Gabor, A. R. Stokes, A. M. Taylor, P. A. Wayman, and W. L. Wilcock. *Principles of Optics: Electromagnetic Theory of Propagation, Interference and Diffraction of Light*. Cambridge University Press, 7 edition, 1999.

[31] John David Jackson. *Classical electrodynamics*. Wiley, New York, NY, 3rd ed. edition, 1999.

[32] William L Barnes. Particle plasmons: Why shape matters. *American Journal of Physics*, 84:593–601, 2016.

[33] `https://www.researchgate.net/publication/277021523_Plasmonic_photocatalysts_of_supported_gold_nanoparticles_for_organic_conversions/figures?lo=1`. (Last visited 06/09/2020).

[34] T. Setälä, A. Shevchenko, M. Kaivola, and A. T. Friberg. Degree of polarization for optical near fields. *Phys. Rev. E*, 66:016615, Jul 2002.

[35] Ravishankar Sundararaman, Prineha Narang, Adam S. Jermyn, William A. Goddard III, and Harry A. Atwater. Theoretical predictions for hot-carrier generation from surface plasmon decay. *Nature Communications*, 5(1):5788, Dec 2014.

[36] Julian Gargiulo, Rodrigo Berté, Yi Li, Stefan A. Maier, and Emiliano Cortés. From optical to chemical hot spots in plasmonics. *Accounts of Chemical Research*, 52(9):2525–2535, 2019. PMID: 31430119.

[37] Shahid Iqbal, Masoud Shabaninezhad, Mohammad Hatshan, Prashanta Niraula, Abubkr Abuhagr, Hasna Alali, Guda Ramakrishna, and Asghar Kayani. Ion-implanted silver nanoparticles for metal-enhanced fluorescence. *AIP Advances*, 8, 09 2018.

Appendix A

Code of basic functions

This appendix merges the mathematical functions needed to calculate scattering coefficients, electric and magnetic fields. Constructing separate functions to call them in the main code could facilitate the calculus and the computing time, as well as keep clear concepts and make easier to search bugs in the program.

The first function called "legendre_p(n)" is able to obtain the associated Legendre polinomials of order 1 and any degree n.

```
function p=legendre_p(n)
    p1=1;
    p2=[1,0];
    if n==0
        p=p1; %P0
    elseif n==1
        p=p2; %P1
    else
        for i=2:n
            p=((2*(i-1)+1)*[p2,0]-(i-1)*[0,0,p1])/i;
            p1=p2;
            p2=p;
        end
    end
end
```

The angle dependant functions π_n and τ_n for any value of n and θ.

```
function PI=legendre_PI(n,theta)
syms x
Pn=poly2sym(legendre_p(n));
Pmn=sqrt(1-(x)^2)*diff(Pn,x);
P=subs(Pmn,x,cos(theta));
PI=P/sin(theta);
end
```

```
function TAU=legendre_TAU(n,theta)
syms x thta
```

```
Pn=poly2sym(legendre_p(n));
Pmn=sqrt(1-(x)^2)*diff(Pn,x);
P=subs(Pmn,x,cos(thta));
tau=diff(P,thta);
TAU=subs(tau,thta,theta);
end
```

Spherical Bessel functions of the first kind j_n and of the third kind $h_n^{(1)}$, which depend on MatLab own Bessel functions. with this, it is also possible to calculate Riccati-Bessel functions and its derivatives.

```
function jn=bessel_j(n,rho)
jn=sqrt(pi/(2*rho))*besselj(n+1/2,rho);
end
```

```
function hn=bessel_h(n,rho)
hn=sqrt(pi/(2*rho))*besselj(n+1/2,rho)+1i*sqrt(pi/(2*rho))*bessely(n+1/2,rho)
    ↪ ;
end
```

```
function dPSI=bessel_dpsi(n,rho)
syms ro
psiro=ro*bessel_j(n,ro);
dpsiro=diff(psiro,ro);
dPSI=subs(dpsiro,rho);
end
```

```
function dCHI=bessel_dchi(n,rho)
syms ro
chiro=ro*bessel_h(n,ro);
dchiro=diff(chiro,ro);
dCHI=subs(dchiro,rho);
end
```

Scattering coefficients a_n and b_n have been calculated by using previous functions.

```
function a=cte_a(n,m,X)
%Bessel para coefs a y b
psimX=m*X*bessel_j(n,m*X);
psiX=X*bessel_j(n,X);
chiX=X*bessel_h(n,X);

dpsimX=bessel_dpsi(n,m*X);
dpsiX=bessel_dpsi(n,X);
dchiX=bessel_dchi(n,X);
%Ctes a y b
 a=(m*psimX.*dpsiX-psiX.*dpsimX)./(m*psimX.*dchiX-chiX.*dpsimX);
end
```

```
function b=cte_b(n,m,X)
%Bessel para coefs a y b
psimX=m*X*bessel_j(n,m*X);
psiX=X*bessel_j(n,X);
chiX=X*bessel_h(n,X);

dpsimX=bessel_dpsi(n,m*X);
dpsiX=bessel_dpsi(n,X);
dchiX=bessel_dchi(n,X);

%Ctes a y b
 b=(psimX.*dpsiX-m*psiX.*dpsimX)./(psimX.*dchiX-m*chiX.*dpsimX);
end
```

Finally, electric and magnetic field are obtained by calling those mathematical functions.

```
function Es=campo_sc(n,X,m,k,r,theta,phi)
rho=k*r;
E0=1;
%Pin y Taun
pin=legendre_PI(n,theta);
taun=legendre_TAU(n,theta);
%Bessel for coefs a & b
psimX=m*X*bessel_j(n,m*X);
psiX=X*bessel_j(n,X);
chiX=X*bessel_h(n,X);
dpsimX=bessel_dpsi(n,m*X);
dpsiX=bessel_dpsi(n,X);
dchiX=bessel_dchi(n,X);
h=bessel_h(n,rho);
%h=((-i)^n)*exp(i*k*r)/(i*k*r);
%Ctes a y b
 a=(m.*psimX.*dpsiX-psiX.*dpsimX)./(m.*psimX.*dchiX-chiX.*dpsimX);
 b=(psimX.*dpsiX-m.*psiX.*dpsimX)./(psimX.*dchiX-m.*chiX.*dpsimX);
%Bessel for modes
dchi=bessel_dchi(n,rho);
%Modes
 Mot=cos(phi)*pin*h; %Theta component of Mo
 Mop=-sin(phi)*taun*h;%Phi component of Mo
 Met=-sin(phi)*pin*h; %Theta component of Me
 Mep=-cos(phi)*taun*h; %Phi component of Me
 Nor=sin(phi)*n*(n+1)*sin(theta)*pin.*h./rho; %Rho component de No
 Not=sin(phi)*taun*dchi./rho;%Theta component of No
 Nop=cos(phi)*pin*dchi./rho;%Phi component of No
 Ner=cos(phi)*n*(n+1)*sin(theta)*pin.*h./rho;%Rho component of Ne
 Net=cos(phi)*taun*dchi./rho; %Theta component of Ne
 Nep=-sin(phi)*pin*dchi./rho;%Phi component of Ne
 Mo=[0 Mot Mop];
```

```
 Me=[0 Met Mep];
 No=[Nor Not Nop];
 Ne=[Ner Net Nep];
 %Electric field
 En=1i^n*E0*(2*n+1)/(n*(n+1));
 Es=En.*((1i*a.*Ne)-(b.*Mo));
end
```

```
function Hs=campo_hsc(n,X,m,k,w,mu,r,theta,phi)
rho=k*r;
E0=1;
%Pin y Taun
pin=legendre_PI(n,theta);
taun=legendre_TAU(n,theta);
h=bessel_h(n,rho);
%Bessel para coefs a y b
psimX=m*X*bessel_j(n,m*X);
psiX=X*bessel_j(n,X);
chiX=X*bessel_h(n,X);
dpsimX=bessel_dpsi(n,m*X);
dpsiX=bessel_dpsi(n,X);
dchiX=bessel_dchi(n,X);
h=bessel_h(n,rho);
%Ctes a y b
 a=(m.*psimX.*dpsiX-psiX.*dpsimX)./(m.*psimX.*dchiX-chiX.*dpsimX);
 b=(psimX.*dpsiX-m.*psiX.*dpsimX)./(psimX.*dchiX-m.*chiX.*dpsimX);
%Bessel for modes
dchi=bessel_dchi(n,rho);
%Modes
 Mot=cos(phi)*pin*h; %Theta component of Mo
 Mop=-sin(phi)*taun*h;%Phi component of Mo
 Met=-sin(phi)*pin*h; %Theta component of Me
 Mep=-cos(phi)*taun*h; %Phi component of Me
 Nor=sin(phi)*n*(n+1)*sin(theta)*pin.*h./rho; %Rho component of No
 Not=sin(phi)*taun*dchi./rho;%Theta component of No
 Nop=cos(phi)*pin*dchi./rho;%Phi component of No
 Ner=cos(phi)*n*(n+1)*sin(theta)*pin.*h./rho;%Rho component of Ne
 Net=cos(phi)*taun*dchi./rho; %Theta component of Ne
 Nep=-sin(phi)*pin*dchi./rho;%Phi component of Ne
 Mo=[0 Mot Mop];
 Me=[0 Met Mep];
 No=[Nor Not Nop];
 Ne=[Ner Net Nep];
 %Magnetic field
 En=1i^n*E0*(2*n+1)/(n*(n+1));
 Hs=En.*((1i*b.*No)+(a.*Me));
end
```